IDENTIFICATION OF SUBMARINE LANDSLIDE FOR TSUNAMI HAZARD ASSESSMENT IN THE GULF OF MEXICO USING A PROBABILISTIC APPROACH

A Thesis

by

LISHA LOHITHAKSHAN PARAMBATH

Submitted to the Office of Graduate and Professional Studies of
Texas A&M University
in partial fulfillment of the requirements for the degree of

MASTER OF SCIENCE

Chair of Committee,	Dr. Juan J Horrillo
Committee Members,	Kuang An Chang
	Prabir Daripa
Head of Department,	Yunlong Zhang

May 2014

Major Subject: Civil Engineering

ABSTRACT

The eastern coast of USA, including the Gulf of Mexico (GOM), is more prone to tsunamis caused by submarine landslides than earthquakes. The Tsunami Hazard Assessment research program lead by ten Brink, 2009, reported the presence of ancient submarine landslides deposit in the GOM dating back to the post glacial period which indicates that there is a likelihood for tsunami events in the future. In fact, the GOM has some of the largest submarine landslides when compared to landslides off the coast of Oregon, central California and New Jersey. Moreover, the high population density and the ongoing industrial development in the GOM, makes it necessary to assess the hazard and develop mitigation plans that involve the development of inundation map, education, early warning and evacuation plans. Specifically in the GOM, assessing the tsunami hazard is to develop tsunami inundation map to identify potential submarine landslide sources, either by using a probabilistic approach or a deterministic approach that uses worst case landslide-tsunami scenarios. A probabilistic approach in the GOM is more suited due to the lack of earlier records of tsunami caused by submarine landslides. Thus the probabilistic model can mimic or create tsunami scenarios based on distribution of physical and geometrical variables involve in the landslide-tsunami mechanisms. Monte Carlo Simulation (MCS) is the tool used to generate random variables under certain distribution, and the MCS Model for the GOM generates a large number of submarine landslides with randomized parameters (like location, runout length, depth, headscarp height, width, slope etc.) capable of producing tsunamis. Parameter results are validated to verify if their distribution follow the same distribution from observed landslide events.

DEDICATION

This thesis is dedicated to my grandfather who was the gentlest of all souls that I have come across in my life. Though Alzheimer's had taken a toll over you, I treasure the moments when you still called me by my name and asked for me. You will be missed forever.

ACKNOWLEDGEMENTS

I would like to express my heartfelt gratitude to Dr. Horrillo for giving me the opportunity to work under him. Your patience and guidance are greatly appreciated. I would also like to thank Dr. Yoshinori for giving me the idea to do this project, and also for his help and support for completing it. I would like to take this opportunity to thank you, and to let you know your help is deeply valued.

I would also like to thank my committee members Dr. Prabir Daripa and Dr. Kuang-An Chang for your valuable feedback and suggestions. I take this opportunity to thank Abhishek and Ju Gao for making this period of my life fun and for your wholehearted support through thick and thin. I would also like to thank Dr. Horrillos family for hosting numerous parties and making every holidays fun-filled. My friends Navya, Aswathi, Sandeep, Reshmi, Nandu and Deepthi who have always found time for me in their life and never thought a second before helping me.

Needless to say, I would like to say I would like to thank my family - my father, mother, brother and Vijisha - for standing by my decisions and for their unquestioning love and support. Last but not the least, my husband Sumesh for being so patient and unquestioning. You all make my life worth living.

TABLE OF CONTENTS

Page

ABSTRACT ii

DEDICATION iii

ACKNOWLEDGEMENTS iv

TABLE OF CONTENTS v

LIST OF FIGURES vii

LIST OF TABLES x

1. INTRODUCTION 1

2. BACKGROUND 5

2.1 Submarine Landslides in the Gulf of Mexico 5
2.2 Selecting Transects in the GOM 7
2.3 Probabilistic Model and Monte Carlo Simulation 9
2.4 Sediment Analysis 14
2.5 Seismic Hazard Map 21
2.6 Translational Slope Failure 21
2.7 Slope Angle and Slide Area 24
2.8 Width of the Submarine Landslide 26
2.9 Landslide Initial Tsunami 28
2.10 Estimation of Return Period 29

3. METHODOLOGY 30

4. RESULTS 35

5. VALIDATION 38

5.1 Comparison of the distribution of input and output parameters . . . 38

5.2 Relation between landslide Volume and Area 38
5.3 Relation between landslide Volume and cumulative number of landslide failures 38

6. CONCLUSION 42

7. FUTURE WORK 43

BIBLIOGRAPHY 44

APPENDIX A. 47

APPENDIX B. 48

LIST OF FIGURES

FIGURE Page

1.1 Bathymetry of the GOM showing the footprint presence of three large submarine landslides East-Breaks landslide, Mississippi Canyon and West Florida landslides in the red-dashed rectangles, Amante (2009). 3

2.1 Bathymetry of GOM showing the variation and the contours of depth 6

2.2 Bathymetry of GOM showing the slope at the continental shelf. . . . 6

2.3 Bathymetry of GOM with the historical submarine landslides. The green circles indicate the size of the landslide in km^3 9

2.4 The map of Gulf of Mexico showing four transects A, B, C and D. . . 10

2.5 Plot of the bathymetric profile along transects A,B,C and D 10

2.6 Probability of observed water depth of landslide having a normal distribution 12

2.7 Probability of observed thickness of landslide having lognormal distribution 13

2.8 Probability of observed length of landslide having lognormal distribution 13

2.9 GOM location and identification of publicly available borehole data . 16

2.10 Classification and characteristics of soil at transect A, (IODP), red : indicate data obtained from site 1319A, black : indicate data obtained from site 1319A 17

2.11 Left: Classification and characteristics of soil at transect B, Right: Borelog at Site 619 18

2.12 Classification and characteristics of soil at transect C, (IODP), red: indicate data obtained from site 1322B, black : indicate data obtained from site 1324B 19

2.13 Classification and characteristics of soil at transect D 20

2.14 GOM Peak Horizontal Acceleration for probability of exceedance of 2% in 50 years.The inset graph shows the hazard curve at location 28.25N, 89.2W which shows the probability of exceedance for 19 values of acceleration expressed as a percentage of g 22

2.15 The components of force involved in translational slope failure, Grilli (2009) 23

2.16 Upper panel: Location of the landslide along transect. Lower Panel: Location of the zoom up showing slope parameters 25

2.17 Empirical relationship between slope angle and slide area obtained from observed data. Fitting line for translation landslides (dashed-red), rotational and blocky landslides (dashed-blue), combined translation and rotational or blocky landslides (dashed-black). 26

2.18 Graph showing the empirical relation between slide area and width of the landslide 27

3.1 Flowchart showing the steps involved in the probabilistic model. . . 31

3.2 Locations at which bulk density and undrained shear strength are determined. 32

3.3 Finding the threshold amplitude by using the best fit curve for the lognormal distribution of the initial amplitude. 34

4.1 Initial wave amplitude generated by submarine landslide for different return period. Red dots represent wave amplitude corresponding to the maximum driving force. 36

4.2 Initial wave amplitude generated by submarine landslide for different return period. Red dots represent wave amplitude corresponding to the maximum amplitude 37

5.1 Probability plot of lognormal distribution of the landslide length generated by the model 39

5.2 Probability plot of normal distribution of the water depth at which the landslide occurs generated by the model 39

5.3 Probability plot of lognormal distribution of the landslide scarp height generated by the model 40

5.4 Relationship between the landslide area and volume of the observed data (left panel) and generated data by the probabilistic model (right panel) 40

5.5 Comparison of slopes for the relationship between landslide volume and cumulative number of landslide failures of both, observed (left panel) and generated data (right panel) 41

A.1 Morphology of a Submarine Landslide 47

B.1 Soil characteristics at Leg 308, Site 1319A 48

B.2 Soil characteristics at Leg 308, Site 1320A 49

B.3 Soil characteristics at Leg 96, Site 619 49

B.4 Soil characteristics at Leg 308, Site 1322B 50

B.5 Soil characteristics at Leg 308, Site 1324B 50

B.6 Soil characteristics at Leg 100, Site 625B 51

B.7 Curve fit for Bulk Density and Undrained Shear Strength at Transect A, B, C and D 52

LIST OF TABLES

TABLE Page

2.1 Details of all the submarine landslides that occurred in the GOM including the various parameters.The last three rows represent the data of East Breaks, Mississippi Canyon and Florida East Breaks landslide respectively. McAdoo (2000); ten Brink (2009) 8

2.2 Distribution of parameters in the GOM 11

2.3 Soil Borelog data 15

1. INTRODUCTION

Tsunami is a series of water waves that are generated as a result of earthquakes, volcanic eruptions, submarine landslides and rarely due to the impact of cosmic bodies (example asteroids, meteorites) in the ocean which results in displacement of large volume of water. The waves thus generated have a large wavelength and a small wave height and as they propagate to the shoreline, where the water depth is shallow, the wavelength reduces and the wave height increases, thereby breaking the wave and resulting in the inundation of the near shore area. Tsunamis are known to cause great threat to the life and property of the coastal communities. Submarine landslides are one of the triggering mechanisms that cause tsunamis. The potential for the occurrence of tsunamis by submarine landslides were recognized more than hundred years back by Milne (1886), but prior to the Papua New Guinea tsunami, most of the tsunamis were thought to be caused due to earthquake sources (Hammack, 1972) . This was mainly due to the fact that there was difficulty in understanding the mechanisms responsible for the occurrence of submarine landslides, in many cases they were thought to be caused by the same trigger mechanisms-earthquake. But the Papua New Guinea Tsunami of 1998 resulted from an earthquake of magnitude 7.0 that took place 25 km off the coast of Aitape, which in turn triggered a landslide-tsunami. The tsunami caused about 2100 deaths, injured thousands, left about 9500 people homeless, and about 500 missing Synolakis (2002). The maximum wave height was estimated at 15 m (59 ft), with an average height of 10m ($\sim$33 ft). Since then, extensive studies have been performed on submarine landslides that cause tsunamis commonly known as tsunami-genic landslides. According to the NGDC Tsunami Event Database NOAA (2008), 73 of the 2275 tsunamis that oc-

curred around the world were caused due to submarine landslides and around 83 % of them, are confirmed to be triggered by earthquakes. In the United States extensive work on tsunamis are being continuously done for the various coastal communities around the United States, so that the hazards can be mitigated. In region where tsunami historical records are limited a common technique is accomplished by using a probabilistic approach. For eastern coast a pioneer study on tsunamis using probabilistic techniques is carried out by Grilli (2009) and similarly in the western coast the studies about probabilistic tsunamis are performed by González (2009).This study in the GOM has been carried out with the assistance of Dr. Yoshinori Shigihara (National Defense Academy of Japan) and Dr.Juan Horrillo (TexasA&M Galveston). The mitigation plan for a tsunami involves a number of steps like the development of a tsunami inundation map which may guide the safety managers to make an evacuation plan, educate the people, etc.

The eastern coast of USA, including the Gulf of Mexico (GOM), is more prone to tsunami-genic landslides than the tsunamis caused by earthquakes.A preliminary 2- D modeling done by Knight (2006) indicated that the sources outside the Gulf are not expected to pose a threat to coastal communities in the GOM. The Tsunami Hazard Assessment Group research program lead by ten Brink (2009), reported the presence of ancient submarine landslides deposit (Figure 1.1) in the GOM dating in the post glacial period which indicates that there is a likelihood for tsunami events in the future. In fact, the GOM has some of the largest submarine landslides when compared to landslides off the coast of Oregon, central California and New Jersey McAdoo (2000). Moreover, the population density and the ongoing industrial development in the GOM, makes it necessary to assess the hazard and develop mitigation plans.

The first step in the tsunami hazard mitigation is the generation of tsunami

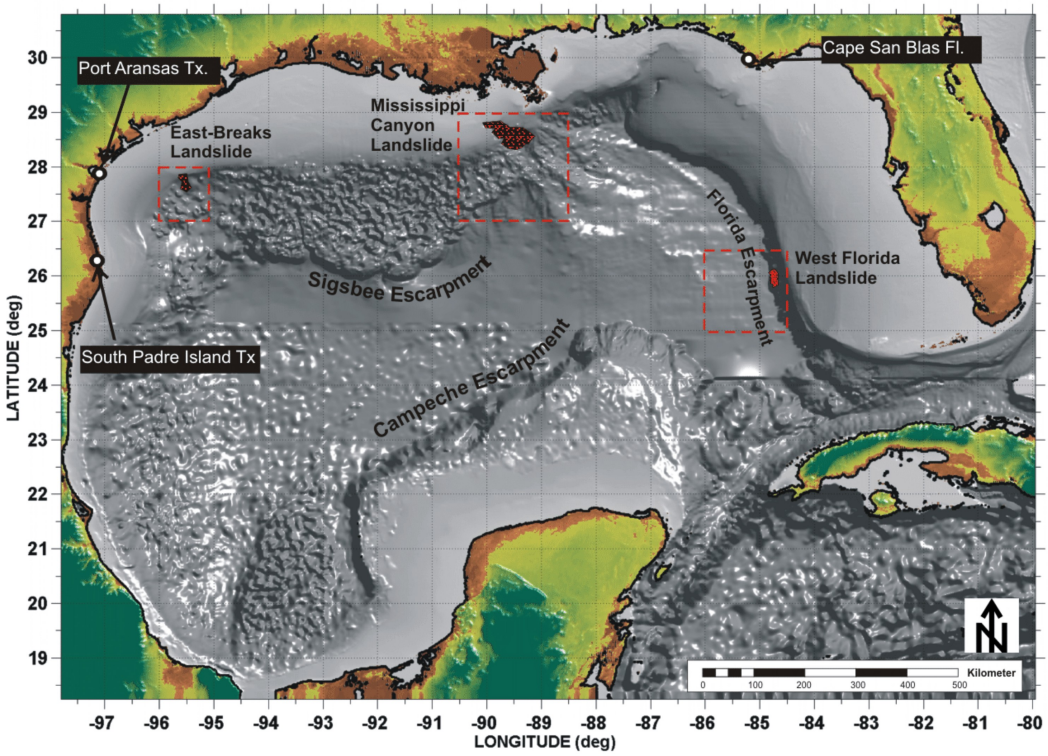

Figure 1.1: Bathymetry of the GOM showing the footprint presence of three large submarine landslides East-Breaks landslide, Mississippi Canyon and West Florida landslides in the red-dashed rectangles, Amante (2009).

inundation map which involves the identification of sources of submarine landslides. Hence a study Horrillo (2010) was done to know the extent of damage that could be caused by the existing submarine landslides like East Breaks, Mississippi Canyon and West Florida, which were identified by ten Brink (2009) and located as shown in the Figure 1.1. The estimation of the inundation elevation and the momentum flux caused by these submarine landslides indicate that they are capable of causing several damages to the coast of GOM. The study based on Port Aransas lying on the coast of GOM Horrillo (2010) indicated that the recurrence of such landslides can cause an average water elevation of 7-13 feet. But the construction of tsunami inundation map with the historical landslides will not give details about any future hazard associated with a recurrence or probability. Hence we need to identify sources

of submarine landslides that have a possibility of occurrence in the future.

In tsunami computational science, a deterministic approach can be used only if the input is known, and consequently, the output produced is always the same. But in a probabilistic approach the use of some degree of randomness in the physical variables involved is a part of the holistic approach. Hence the assessment of tsunami in the GOM can be done either by using a probabilistic approach Lynett (2012); Grilli (2009); González (2009) or deterministic approach Priest (2009) that uses worst case landslide-tsunami scenarios. A probabilistic approach for identification of landslide sources is more suited in the GOM due to the lack of earlier records of tsunamis caused by submarine landslides. Monte Carlo Simulation (MCS) is the tool that is used in the probabilistic approach to generate random variables confined or limited under certain distribution; and it is also used in solving problems that have aleatory or cognitive uncertainties Ang (2007).

This thesis discusses the identification of landslide tsunami sources in the GOM, using a probabilistic model developed with MCS, the results of which can be used later for creating tsunami inundation maps for the GOM. The chapter 2 and 3 in this thesis elaborates the theory and the methodology used to develop the probabilistic model. The results obtained from the model are listed under chapter 4. Every step in the probabilistic model is validated and the validation for the model is discussed in chapter 5. The chapter 6 and 7 gives the conclusion and the scope of future study.

2. BACKGROUND

The common triggering mechanisms of submarine landslides that results in tsunami are earthquakes, slope over steepening, overpressure due to rapid deposition of sediments, presence of weak soil layers, wave loading on sea bottom by storms or hurricanes, build up of excess pore water pressure gas hydrate dissociation by change of temperature or pressure, ground water seepage (Hampton and Locat,1996). The study of submarine landslides is continued in the shelf break which is located between the abyssal plain and the continental shelf. Figure 2.1 shows the isobath and shelf break of the GOM.The shelf break is a continental slope which is largely formed by the deposition of sediments carried down by the existing and ancient rivers. As the deposition of sediment at the slope increases, it becomes unstable which in turn results in the failure of slope.

The submarine landslides are also caused when the soil sediments on the slope are affected by a seismic activity that takes place underneath the water body.The Figure 2.2 shows the slope in the Gulf of Mexico that is determined by using Arc GIS 10 using the 'slope' tool. In the GOM, as seen from the Figure 2.2 the continental slopes are very gentle mostly ranging from 1 to 5 degrees. Under this consideration the most probable occurrence of a submarine landslide is one that is caused by earthquake or seismic activity. Therefore this study is based on submarine landslides that are triggered by a seismic activity.

2.1 Submarine Landslides in the Gulf of Mexico

A morphometric study of the submarine landslides in the GOM was done by McAdoo et al. (2000), wherein they identified the submarine landslides in various locations off the coast of United States using multibeam bathymetry and GLORIA

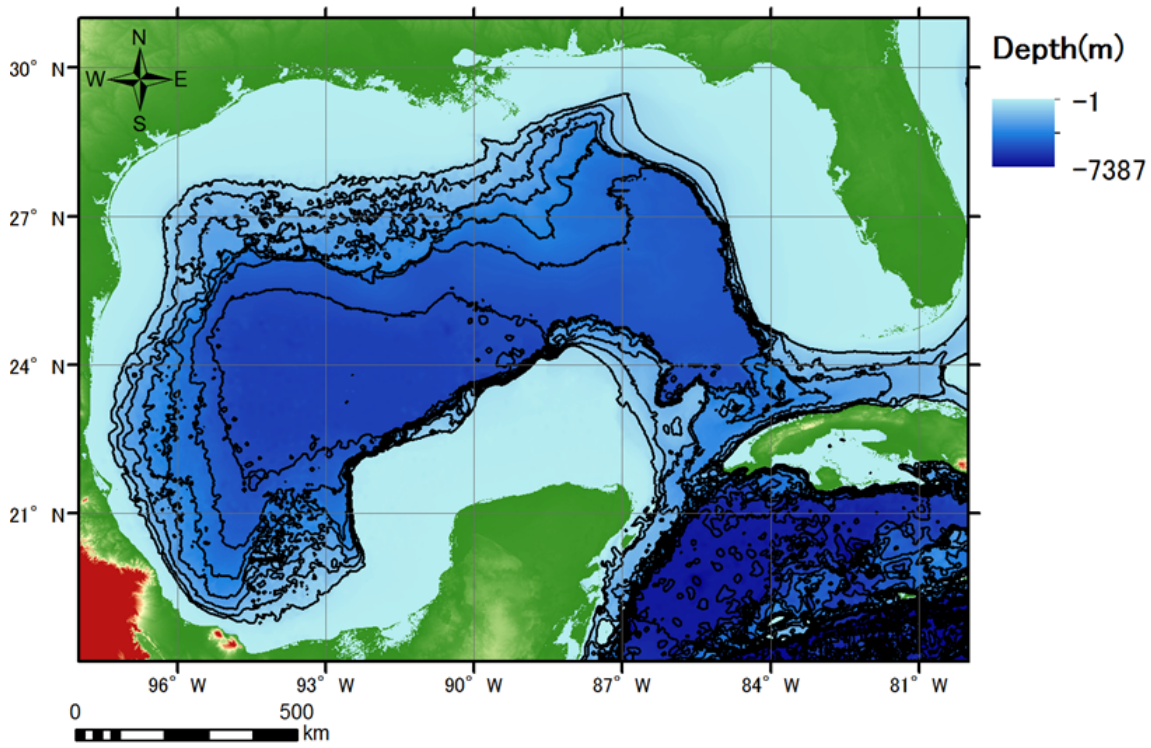

Figure 2.1: Bathymetry of GOM showing the variation and the contours of depth

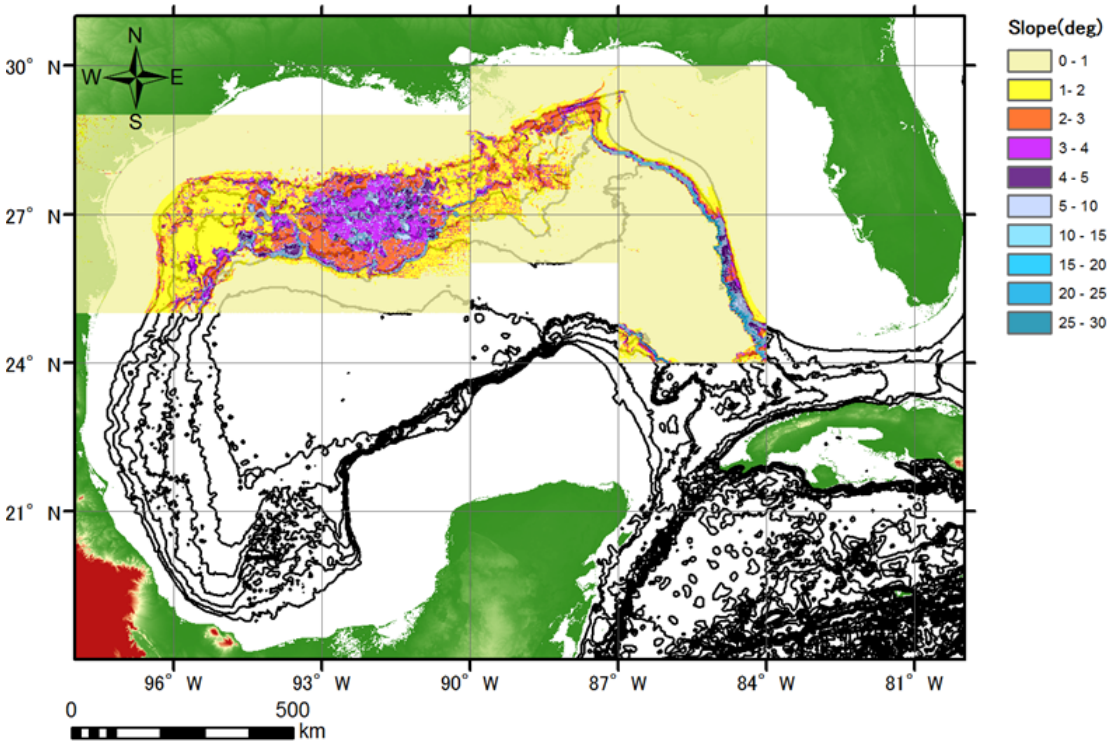

Figure 2.2: Bathymetry of GOM showing the slope at the continental shelf.

side scan survey. Thus important aspects of the submarine landslides like the location, area, depth of headscarp, runout length, width, unfailed adjacent slope, slide volume, etc. were determined in a time and cost effective method . The characteristic of the landslide specifying all the features listed above is in Appendix A. One of the most important inferences of this study is that submarine landslides in the GOM take place in slopes of 11.5 ° or lesser. Another conclusion drawn from the study is the that slope of landslides having bigger runout length was small and the slope of landslides having smaller runout length was big. These conclusions also show that the landslides taking place here are primarily triggered by the seismic activity than by the instability of the slopes. In addition to this, another study by ten Brink (2009) showed the presence of three more submarine landslides namely the East Breaks, The Mississippi Canyon and the Florida Escarpment as shown by Figure 1.1. The Mississippi Canyon landslide is considered to be the largest and the latest and is dated to be 7,500 to 11,000 years. As the Mississippi river continues to discharge sediments into the GOM, there is a possibility of recurrence of such submarines landslides due to slope failure caused by the overburden of these sediments. Table 2.1 shows the details of all the submarine landslides that occurred in the GOM including the various parameters used to characterize the landslides and Figure 2.3 shows the isobath in the GOM and it also illustrates the location and the size of the historical submarine landslides in the GOM. From the Figure 2.3 it is evident that the landslides occur at the shelf break where there is a gradient of depth.

2.2 Selecting Transects in the GOM

The probability analysis in the GOM is carried out along specified transects in the GOM.These transects are chosen such that they lie across the location for which bore hole data are available, making it easier to select soil properties across the

Table 2.1: Details of all the submarine landslides that occurred in the GOM including the various parameters.The last three rows represent the data of East Breaks, Mississippi Canyon and Florida East Breaks landslide respectively. McAdoo (2000); ten Brink (2009)

No	Lat.	Long.	Type	Area	HS depth	RO length	Width	W/L	Adj	HS height	Slide	T/l	Volume
	(°)	(°)		$A(km^2)$	d (m)	l (km)	(km)		slope(°)	T (m)	Vol. (km^3)	unitless	km^3
1	26.25	-93.00	Disint.	452.0	-1918	49.0	9.22	0.2	1.1	60.0	8.9	0.00122	13.56
2	27.42	-92.49	Slump	44.0	-1423	3.8	11.58	3.0	2.1	140.0	2.0	0.03684	3.08
3	27.39	-92.37	Disint.	29.0	-1469	12.0	2.42	0.2	3.0	111.7	1.1	0.00931	1.62
4	27.4	-92.27	Slump	62.0	-1356	12.0	5.17	0.4	3.1	148.3	3.0	0.01236	4.60
5	27.3	-92.19	Disint.	48.0	-1301	5.5	8.73	1.6	5.5	75.0	1.2	0.01364	1.80
6	26.67	-92.26	Disint.	52.0	-2024	14.0	3.71	0.3	5.0	200.0	3.4	0.01429	5.20
7	26.67	-92.19	Blocky	15.0	-1874	8.8	1.70	0.2	11.5	160.0	0.8	0.01818	1.20
8	26.28	-92.14	Disint.	15.0	-2053	8.6	1.74	0.2	1.1	110.0	0.5	0.01279	0.83
9	26.36	-91.98	Disint.	10.3	-2019	3.0	3.43	1.1	6.0	203.3	0.7	0.06777	1.05
10	26.74	-91.61	Disint.	1156.0	-2150	79.0	14.63	0.2	NaN	263.3	100.4	0.00300	152.19
11	27.29	-91.41	Blocky	9.6	-1757	4.9	1.96	0.4	12.0	160.0	0.5	0.03265	0.77
12	27.11	-91.41	Disint.	34.0	-1733	7.6	4.47	0.6	2.5	60.0	0.7	0.00789	1.02
13	27.94	-91.32	Blocky	143.0	-1076	12.0	11.92	1.0	5.0	176.3	8.3	0.01469	12.61
14	26.21	-91.19	Disint.	28.0	-2399	7.3	3.84	0.5	5.1	191.7	1.8	0.02626	2.68
15	27.79	-91.18	Blocky	42.0	-1332	6.8	6.18	0.9	8.1	172.5	2.4	0.02537	3.62
16	28.03	-90.95	Disint.	70.0	-910	5.8	12.07	2.1	3.1	146.7	3.4	0.02529	5.13
17	26.51	-90.88	Disint.	148.0	-2262	12.0	12.33	1.0	7.5	315.0	15.1	0.02625	23.31
18	26.72	-90.72	Disint.	55.0	-2395	7.1	7.75	1.1	9.9	255.0	5.6	0.03592	7.01
19	27.9	-90.54	Disint.	40.0	-1091	4.2	9.52	2.3	4.4	161.3	2.1	0.03840	3.23
20	27.57	-90.24	Disint.	748.0	-1404	45.0	16.62	0.4	1.0	55.0	13.6	0.00122	20.57
21	27.46	-90.04	Disint.	5509.0	-2328	167.0	32.99	0.2	1.3	53.8	97.7	0.00032	148.19
22	28.01	-89.42	Disint.	1394.0	-2228	79.0	17.65	0.2	1.6	73.8	33.9	0.00093	51.44
23	29.1	-88.93	Disint.	2913.0	-1136	124.0	23.49	0.2	2.0	48.3	46.4	0.00039	70.35
24	29.95	-87.64	Disint.	2460.0	-1414	111.0	22.16	0.2	1.3	97.5	79.1	0.00088	119.93
25	30.87	-87.02	Disint.	1098.0	-121	89.0	12.34	0.1	1.9	60.0	13.1	0.00067	32.94
26	27.71	-94.69	Disint.	519.0	-150	39.0	13.31	0.3	1.1	160.0	22.0	0.00410	21.95
27	28.51	-89.78	Disint.	3687.0	-250	145.0	25.43	0.2	1.0	300.0	425.0	0.00207	425.00
28	26.09	-84.75	Disint.	647.0	-800	19.0	34.05	1.8	5.8	150.0	16.2	0.00789	16.20

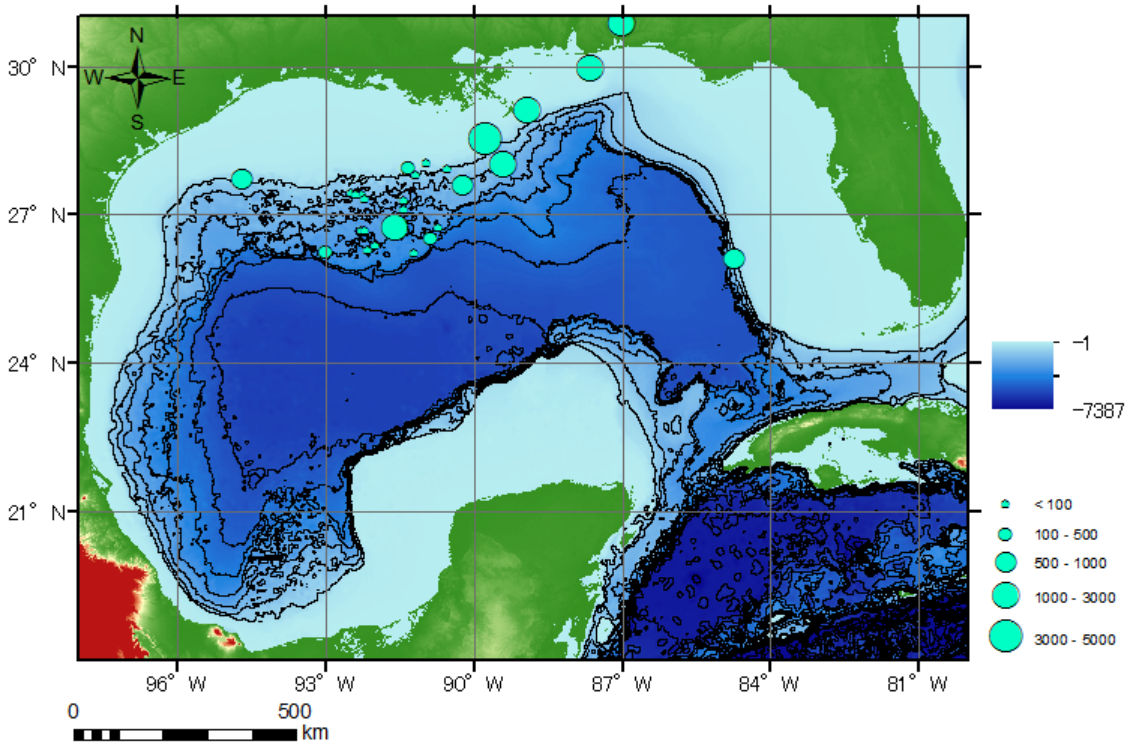

Figure 2.3: Bathymetry of GOM with the historical submarine landslides. The green circles indicate the size of the landslide in km^3

transects. The criterion for transects' direction is that, they should lie perpendicular to the bathymetry contours as a landslide follows the shorter downslope path. The transects are identified on Figure 2.4 as 'A','B','C' and 'D'. Once the transects are selected the bathymetry profile along the transect is obtained. The Figure 2.5 gives the bathymetric profile at each of the transects. From the Figure 2.5 we observe that the slopes along each of these transects is very gentle ranging from 1.55° to 1.56°

2.3 Probabilistic Model and Monte Carlo Simulation

Probability in general is defined as the numerical measure of the likelihood of occurrence of an event by incorporating the exhaustive set of all possible alternative

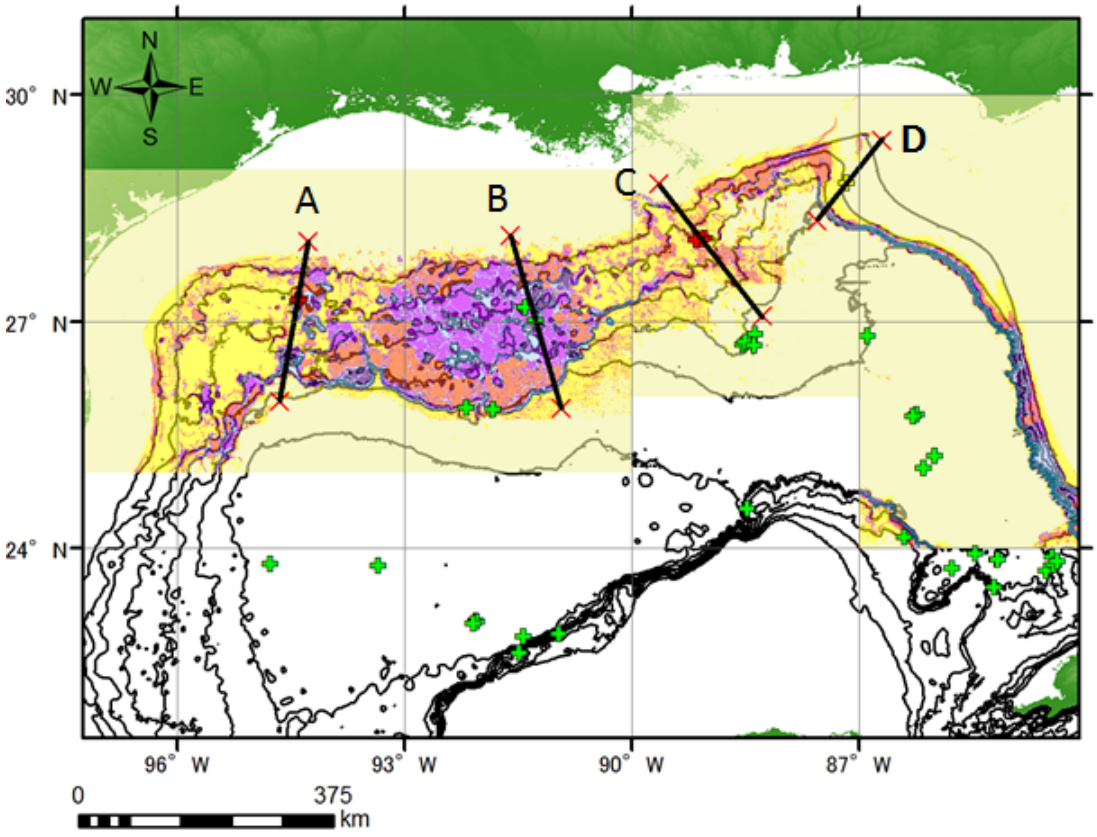

Figure 2.4: The map of Gulf of Mexico showing four transects A, B, C and D.

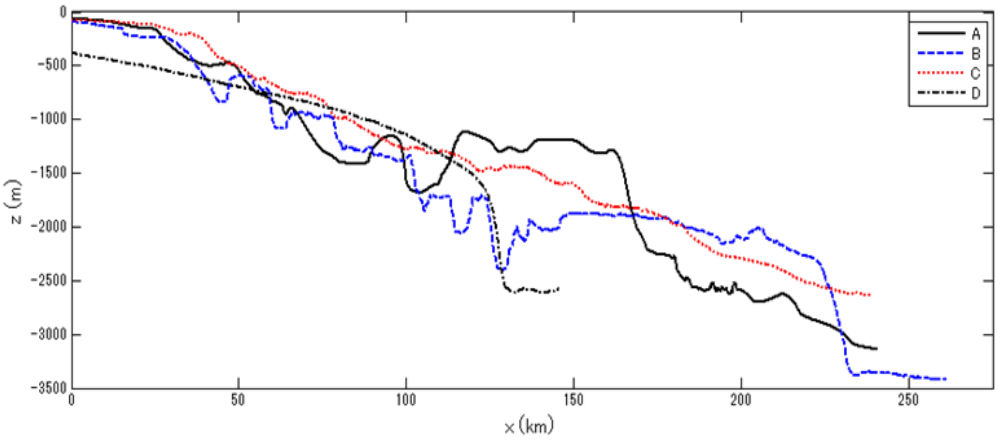

Figure 2.5: Plot of the bathymetric profile along transects A,B,C and D

events. Hence the first step in creating a probabilistic model is to identify the event of interest and assign the set of all probabilities for the event. Monte Carlo Simulation (MCS) is a tool that helps to model problems that have certain level of uncertainty. The first step of the MCS for the GOM is to identify landslide parameters for a tsunami-genic event (example length, depth and thickness) from the known sources and find the distribution they follow within the domain (GOM). Then, random variables are generated for these parameters so that they follow their respective distribution over this domain. The randomly generated parameters are used for deterministic computations of stability analysis and tsunami wave height. Since the parameters are randomly generated each time the model generates slightly different values. Hence this process is repeated a number until a considerable number of landslide -tsunami events are obtained .

Results are examined and valuated to match the distribution of the random parameters. The parameters that are examined in the GOM basin for the translational slope failure are the water depth (d) at which scarp is located, the length of landslide (l) and the thickness of the landslide (T). Table 2.2 gives the details of the parameters that are used for generating the random variable in the MCS. Random variables are limited within the maximum and minimum of the observed values.

Table 2.2: Distribution of parameters in the GOM

SI No.	Parameter	Unit	Distribution	μ	σ	Max.	Min.
1	Depth (d)	m	Normal	1559.76	735.642	121	2399
2	Length (l)	km	Lognormal	3.14	1.337	3	167
3	Thickness (T)	m	Lognormal	4.7788	0.63	48.3	315

According to the observed values in the GOM (McAdoo (2000) and ten Brink

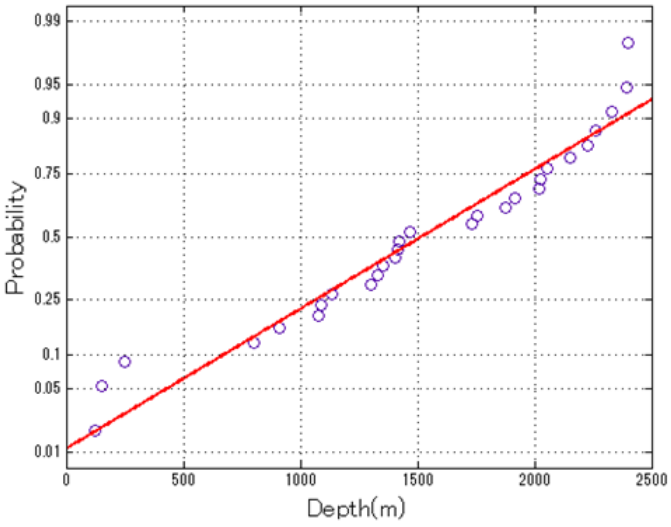

Figure 2.6: Probability of observed water depth of landslide having a normal distribution

(2009)) the water depth (d) at which the landslide occurs follows a normal distribution as shown in the Figure 2.6. The randomly generated values of d are based on the mean (μ) and the standard deviation (σ) which are the statistical parameters of the normal distribution of the observed data. The depth is randomly generated using the 'normrnd' function in MATLAB as follows:

$$d = normrnd(\mu_d, \sigma_d)$$

The thickness and length of observed values of landslide in the GOM follow a lognormal distribution as shown in the Figure 2.7 and 2.8. The statistical parameters μ and σ of a lognormal distribution is defined by the following equations.

$$\mu = \log\left(m^2/\sqrt{(v+m^2)}\right) \tag{2.1}$$

$$\sigma = \sqrt{\log\left(v/m^2+1\right)} \tag{2.2}$$

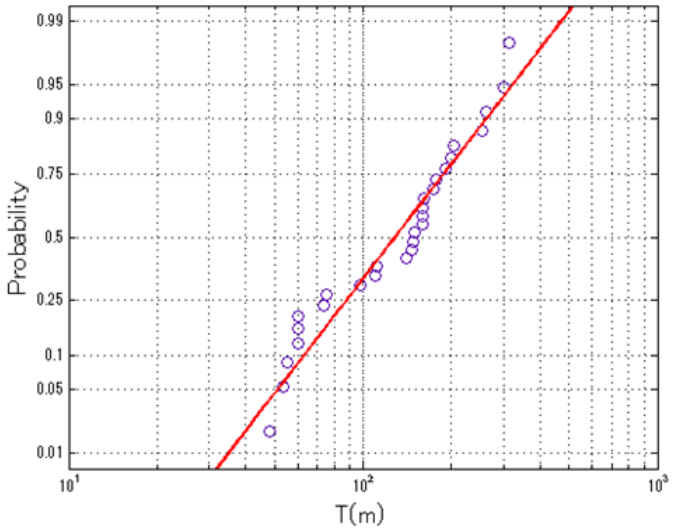

Figure 2.7: Probability of observed thickness of landslide having lognormal distribution

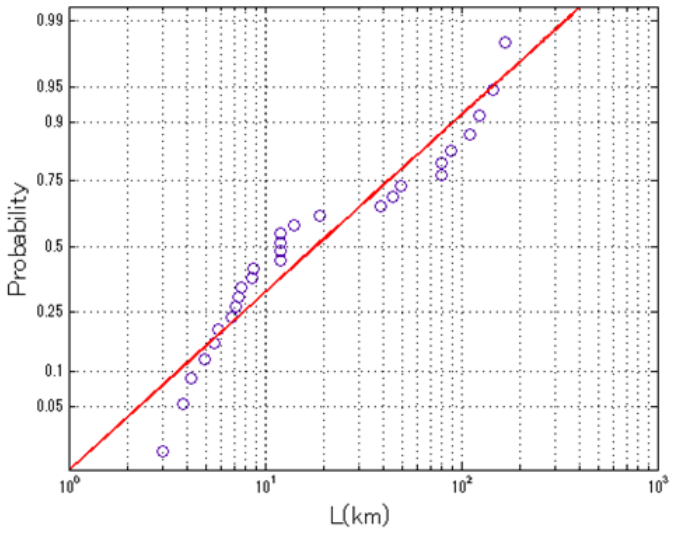

Figure 2.8: Probability of observed length of landslide having lognormal distribution

where m and v are the mean and variance of the observed values of T and l. The thickness and length of the landslide is randomly generated using the MATLAB 'lognrnd' function as follows:

$$T = logrnd(\mu_T, \sigma_T)$$

$$l = logrnd(\mu_l, \sigma_l)$$

The generated parameters d, l and T are used to calculate the slope, area, width and initial amplitude of the wave. But since the parameters are randomly generated each time the model generates different value of data each time.Therefore, a large number of runs are needed for convergence and consistent results. According to Nowak and Collins, (2000) the convergence of a MCS model can be determined using,

$$P_{max} = \frac{1}{(NCoV^2) + 1} \tag{2.3}$$

where N is the number of simulations,Cov is the coefficient of variation for the study and P_{max} is the maximum probability of exceedance that can be predicted by the model.

In this study, the probabilistic model is used to estimate a probability of exceedance of 0.0001 (or a return period of 10,000 years) with a maximum coefficient of variation to be 10%. Hence the number of simulations to be carried out for each transect will be $999,900$, which can be rounded off to $1,000,000$ trials on each transect.

2.4 Sediment Analysis

In the GOM there are publicly available borelog data recorded and generated by several sources and agencies like Integrated Ocean Drilling Program(IDOP), Ocean Drilling Program (ODP) (dated from 1984-1989)and Deep Sea Drilling Project (DSDP) (dated from 1968-1983), which are distributed at various locations in the

Gulf as shown in the Figure 2.9. The data which are used in this study and the format in which they are available are as given in Table 2.3 as follows :

Table 2.3: Soil Borelog data

Source	Site	Transect	Format
Integrated Ocean Drilling Program -	Leg308, Site1319A&1320A	A	Digital
(IODP)	Leg308, Site1322B&1324B	C	Digital
Ocean Drilling Program - (ODP)	Leg100, Site625B	D	Not Digital
Deep Sea Drilling Project -(DSDP)	Leg96, Site619	B	Not Digital*

* Bulk density data has been digitized

The location of these boreholes with the detailed soil characteristics is given in Appendix B.

The IDOP Leg 308 site 1319A and 1320 are used to depict the soil characteristics at transect A. From Figure 2.10 both the borelog portray similar characteristics of the soil. Most of the data are categorized as fine grained, cohesive material, under undrained loading condition.

Based on the lithology of DSDP Leg96, Site619 at transect B shown in Figure 2.11, most characteristic type of soil found is clay or mud, that is fine grained, cohesive and under undrained loading condition. Transect C is also represented by 2 bore hole data IDOP Leg308, Site1322B and 1324B as shown in Figure 2.12. Both the bores have similar characteristics for soil properties. From the Figure 2.12, it can be concluded that the soil at transect C is fine grained, cohesive and under undrained loading condition. For transect D (Figure 2.12) based on the classification of soil on lithology it is found to mainly have mud and silt or clay.

The inferences drawn based on the borehole data presented, shows that the sediments in the GOM are largely comprised of clay or mud which are mostly cohesive.

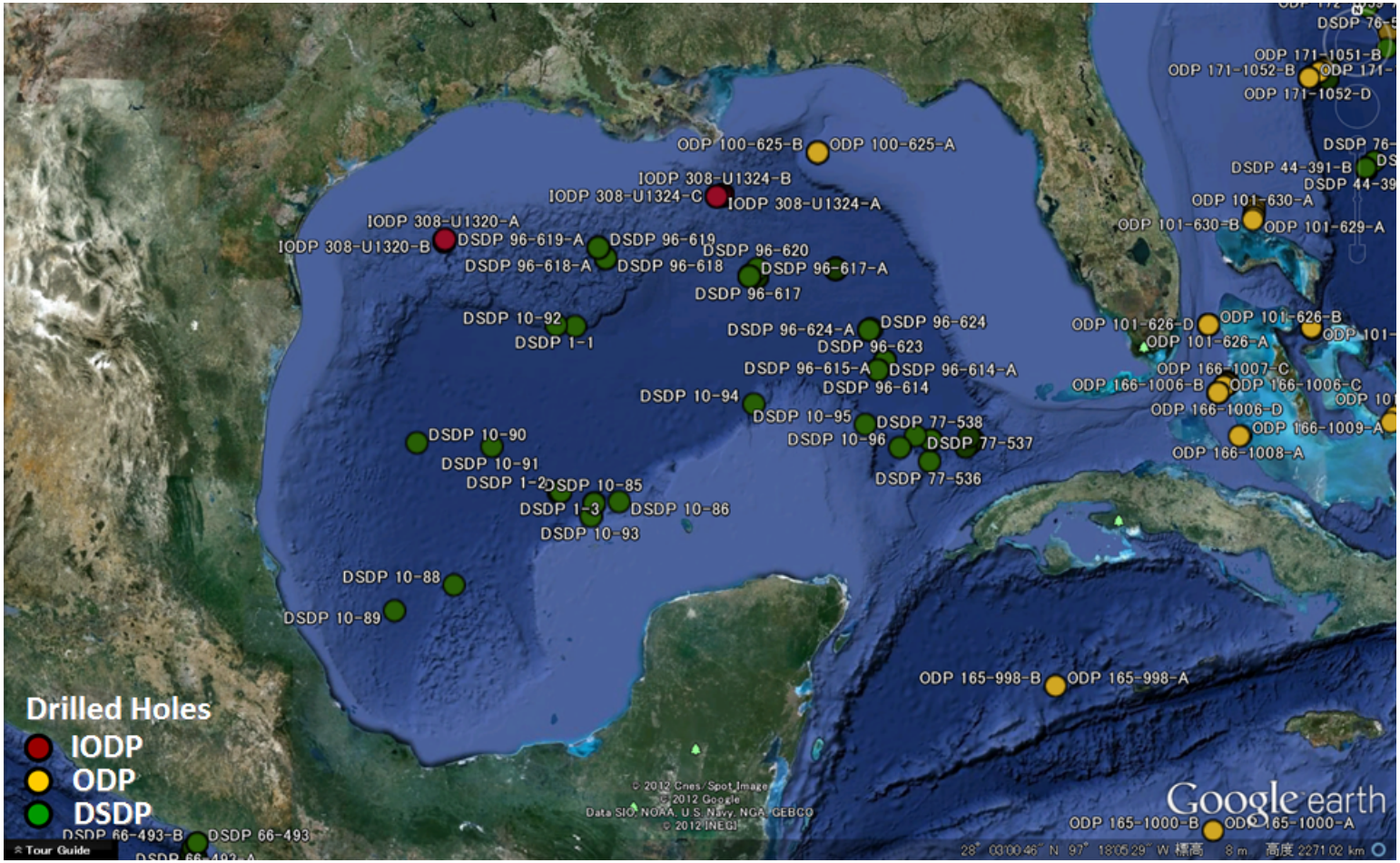

Figure 2.9: GOM location and identification of publicly available borehole data

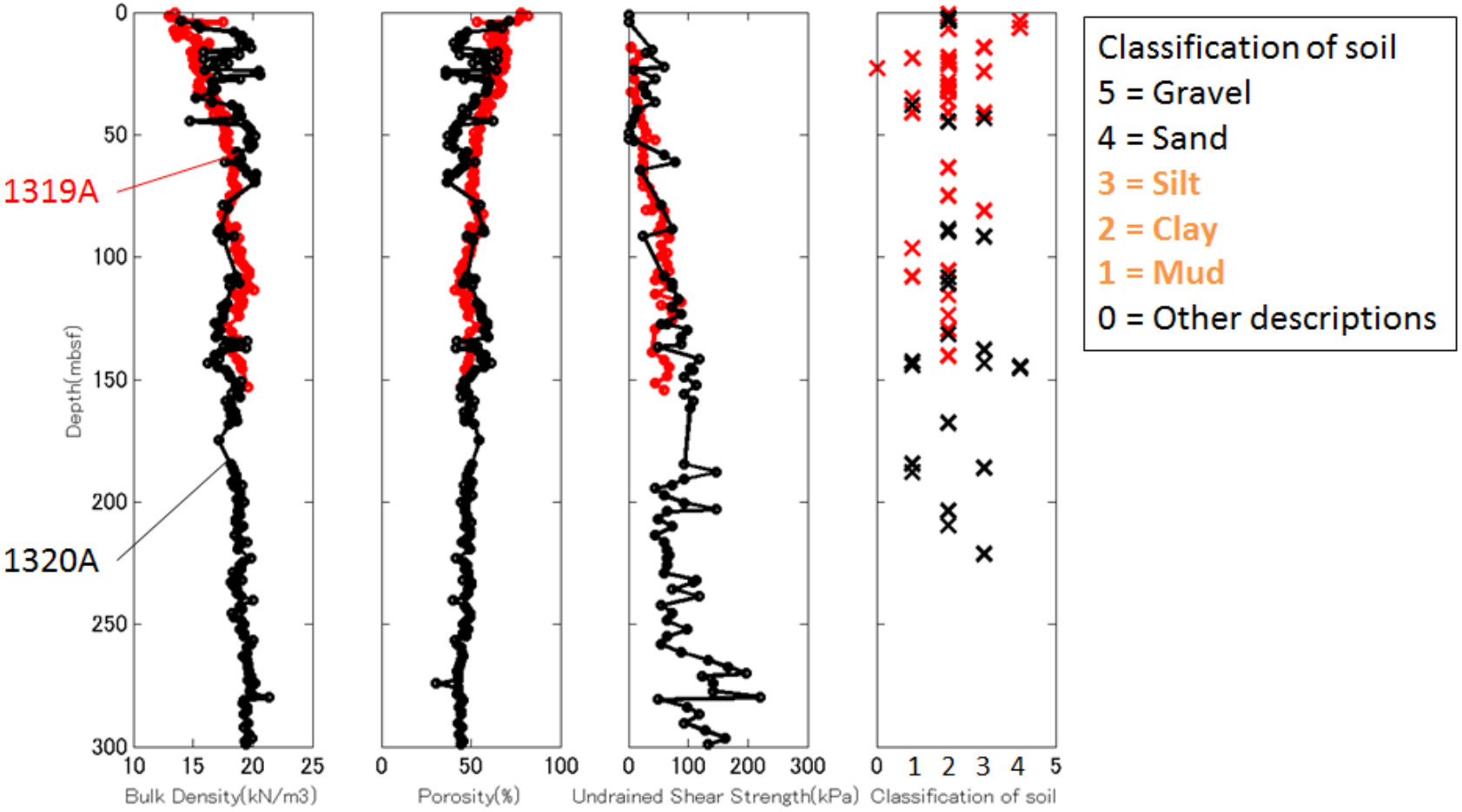

Figure 2.10: Classification and characteristics of soil at transect A, (IODP), red : indicate data obtained from site 1319A, black : indicate data obtained from site 1319A

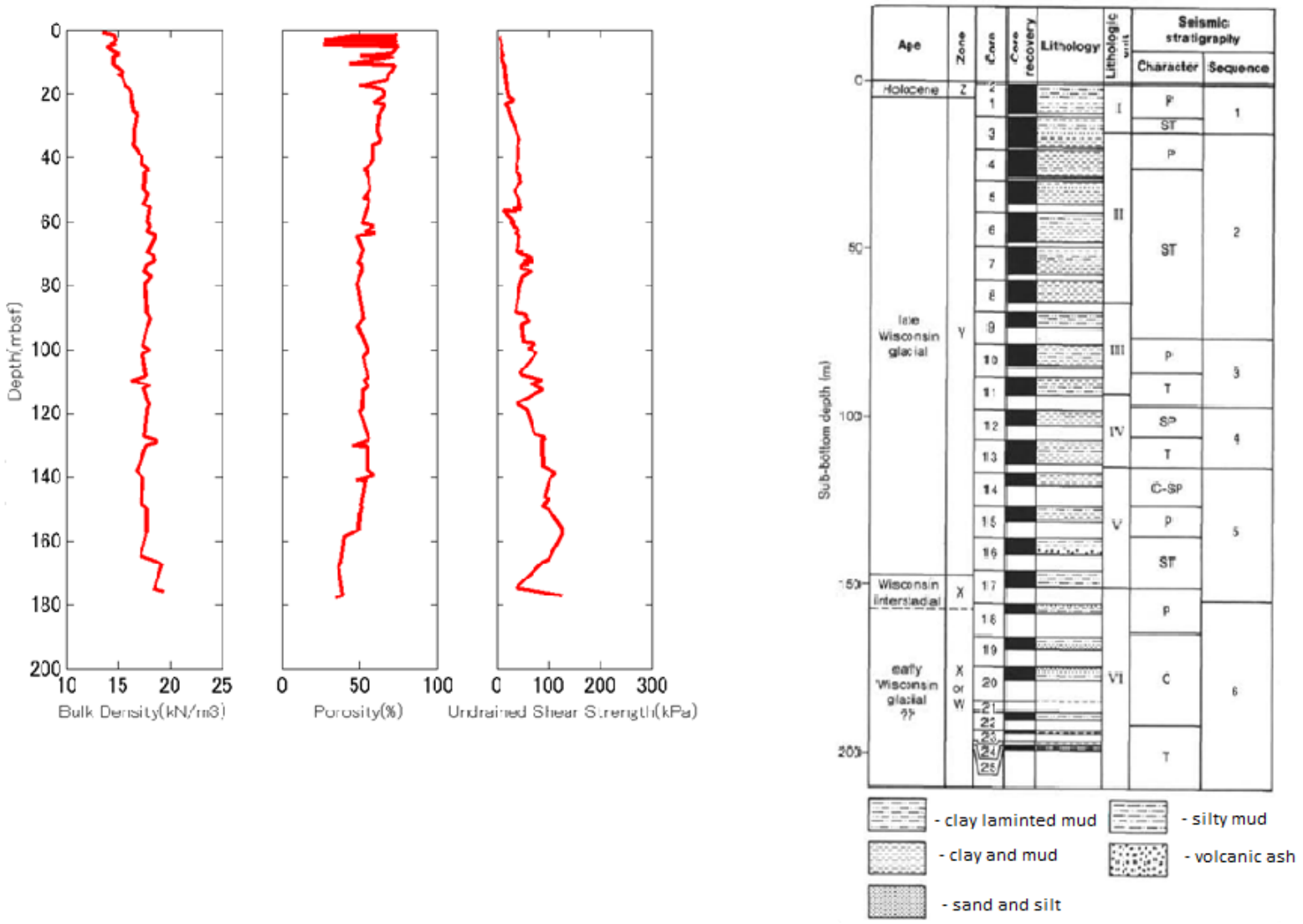

Figure 2.11: Left: Classification and characteristics of soil at transect B, Right: Borelog at Site 619

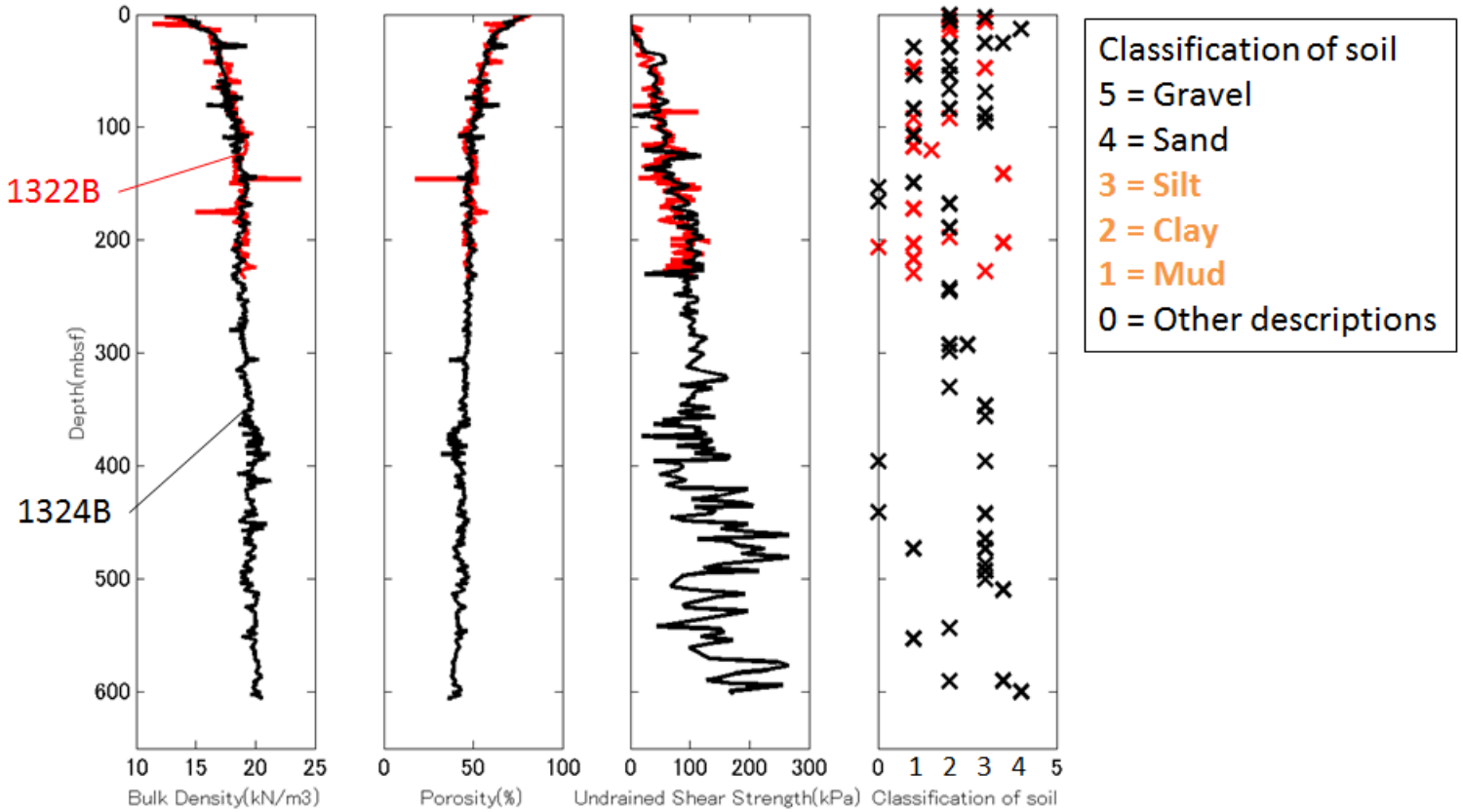

Figure 2.12: Classification and characteristics of soil at transect C, (IODP), red: indicate data obtained from site 1322B, black : indicate data obtained from site 1324B

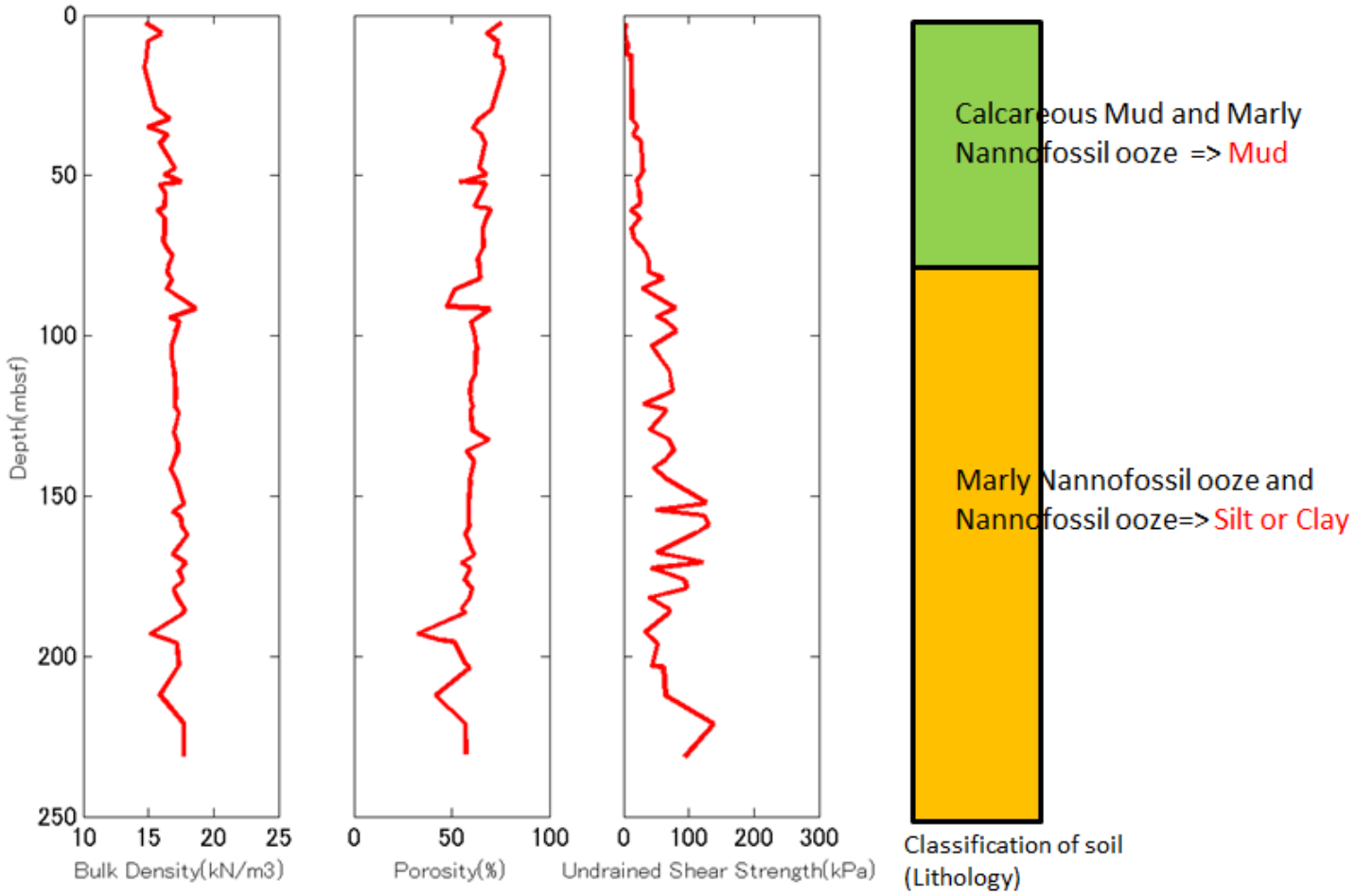

Figure 2.13: Classification and characteristics of soil at transect D

2.5 Seismic Hazard Map

The US Geological Survey (USGS) published the National Seismic Hazard Map in 2008 that compile all the earthquake Peak Horizontal Acceleration for various probability levels across the United States Mar.D Peterson et al., (2008). The Seismic Hazard Map of the GOM is included in the database. Each point in the hazard map represents the probability of exceedance corresponding to nineteen intensities of horizontal acceleration. The Figure 2.14 the Peak Horizontal Acceleration (PHA) expressed as a percentage of acceleration due to gravity (g) for the GOM that correspond to the 2% in 50 year probability of exceedance. The reciprocal of the probability of exceedance gives the return period. Notice that the Figure 2.14 the inset graph represents the plot of the probability of exceedance to the log of acceleration at the location (28.25N, 89.2W). In the slope stability analysis the PHA value is incremented for various annual rate of exceedance or return period (like 50, 100, 150, ...10,000) at the location of the landslides, and the probability of exceedance at when the slope fails is taken as the point at which seismic activity can be triggered.

2.6 Translational Slope Failure

Submarine landslides are classified into two namely the translational and rotational landslides, Locat and Lee,(2002). Translational landslides are the most common events in the GOM. Most of them occurs on very mild slopes and shallow depth, whereas the rotational landslides occur on concave surfaces of failure when overburden forces overcome the resistive forces. 80% of all submarine landslides that took place in the GOM are caused due to translational slope failure. As stated earlier, in the GOM the failure of submarine landslides are assumed to be triggered by earthquakes, hence the instability analysis will include a component PHA of the seismic activity. Since there is a dynamic component contributed by the PHA of earthquake

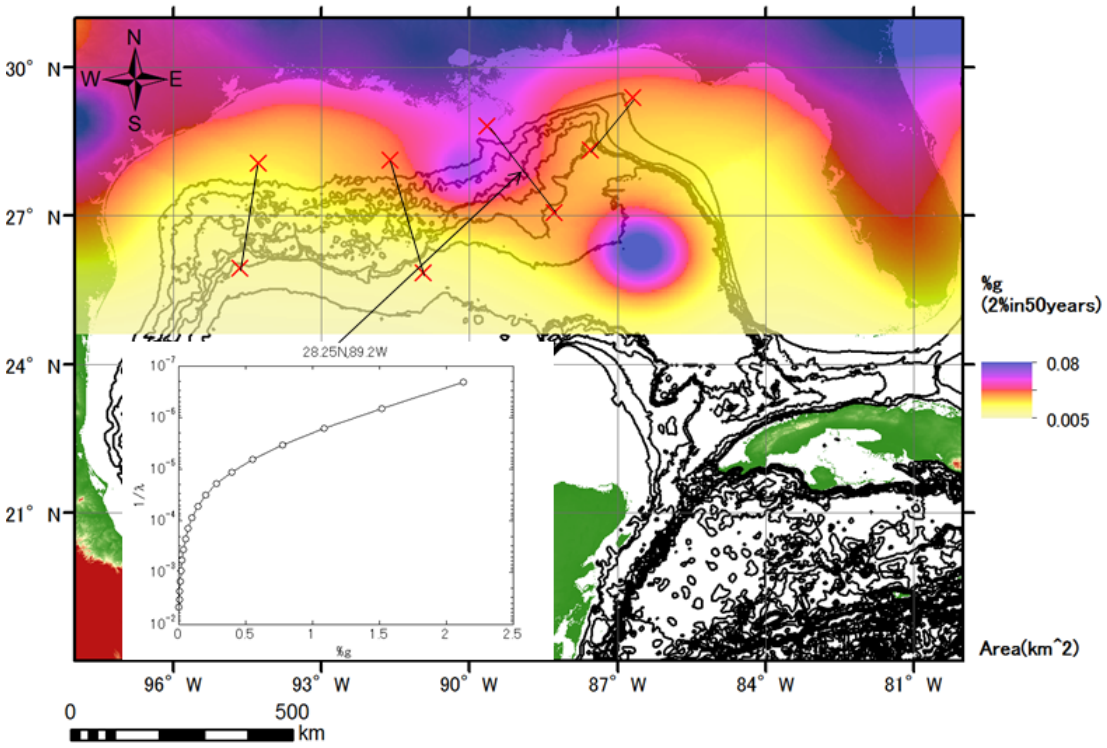

Figure 2.14: GOM Peak Horizontal Acceleration for probability of exceedance of 2% in 50 years.The inset graph shows the hazard curve at location 28.25N, 89.2W which shows the probability of exceedance for 19 values of acceleration expressed as a percentage of g

we use a quasi-static method for analysis of stability of translational landslides. If we consider a translational slope as given below in Figure 2.15, Grill et al. (2009), a slope failure will occur when the sum of all driving force is greater than the sum of all resistive force. Hence when the factor of safety (FS), which is the ratio of the sum of all resistive forces to the sum of all driving force, is less than unity, a slope failure will occur. For a translational slope failure the FS is calculated using the equation,

$$FS = \frac{c' + \sigma' \tan \Phi}{\tau_d}, \tag{2.4}$$

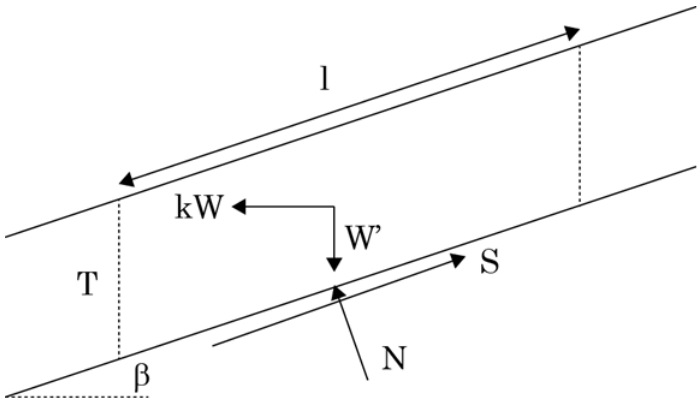

Figure 2.15: The components of force involved in translational slope failure, Grilli (2009)

where c' is the effective cohesion of the sediment, Φ is the effective angle of internal friction,σ' is the effective normal stress, τ_d is the shear stress and . The normal stress (σ') and the shear stress (τ_d) are obtained by computing the normal force (N) and the shear force (S) per unit area of a failure plane of unit width respectively. The expression for N and S is obtained as follows:

$$N = W' \cos\beta - kW \sin\beta \tag{2.5}$$

$$S = W' \sin\beta + kW \cos\beta \tag{2.6}$$

where W is the total weight of the landslide per unit width ;hence $W = \rho_s glT$, W' is the buoyant weight of landslide; hence $W' = (\rho_s - \rho_w)glT$, ρ_s is the bulk density of the soil, ρ_w is the density of water and k is the seismic coefficient defined as PHA/g.

Since the sediments along the transects A, B, C, D are clayey soil the angle of internal friction(ϕ) can be considered equal to zero. As the effective cohesion of the soil is equal to the undrained shear strength (S_u) in the case of clayey soil, the

equation for the factor of safety is obtained as

$$FS = \frac{S_u}{(\rho_s - \rho_w)gT \sin\beta + k\rho_s T \cos\beta}. \tag{2.7}$$

The geometric parameters like landslide thickness(T) and length (l) are randomly generated using the MCS. As stated earlier, the stability of the slope along any transect is is tested for ascending values of k for different return period until FS is less than one. The return period, at which the FS is less than one, is used later for the calculation of probability of exceedance of PHA.

2.7 Slope Angle and Slide Area

The slope of the landslide is obtained at the randomly generated location on the transect profile. When a randomly generated water depth(d) and l of the landslide is obtained by MCS, the parameters d_1, l_1, d_2 and l_2 can be determined as shown in Figure 2.16. The slope at the transect β is calculated as

$$\beta = \arctan\left(\frac{d_2 - d_1}{l_2 - l_1}\right) \tag{2.8}$$

When the slope of the landslide is found, the slide area can be determined from the empirical relationship between the slope angle and the slide area obtained from the observed data of landslides in the GOM, see Figure 2.17 . The Figure 2.17 shows the relationship between the translational and the rotational or blocky slides with the slope angle for the observed data and an empirical relation is obtained by fitting a line to the relation. Therefore, the empirical relation between the area and the

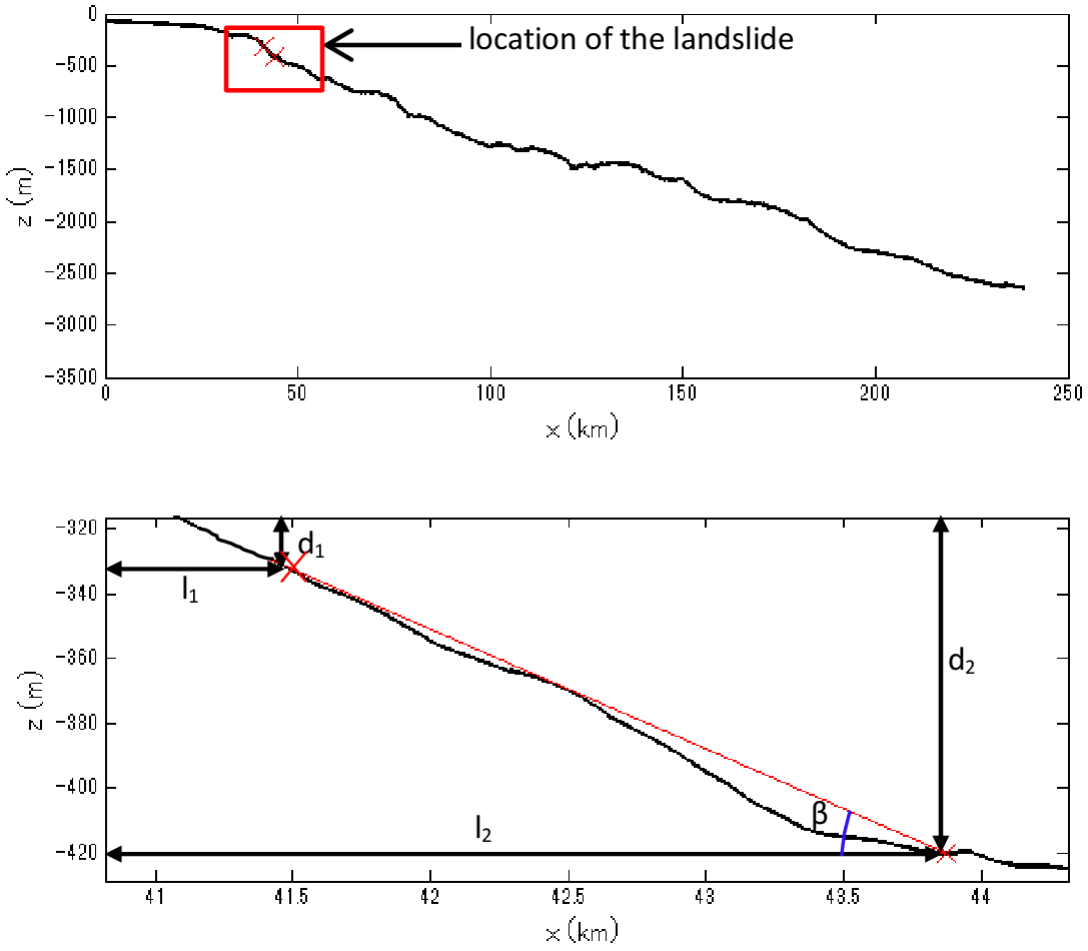

Figure 2.16: Upper panel: Location of the landslide along transect. Lower Panel: Location of the zoom up showing slope parameters

slope angle of a translational landslide is given by,

$$A = \left(\frac{7.094 - \beta}{1.358}\right)^{5.462} \tag{2.9}$$

where A is the area of the landslide in km^2 and β is the angle of the slope in degrees. Notice on Figure 2.17, there are no values of slope angle less than 10 km^2.

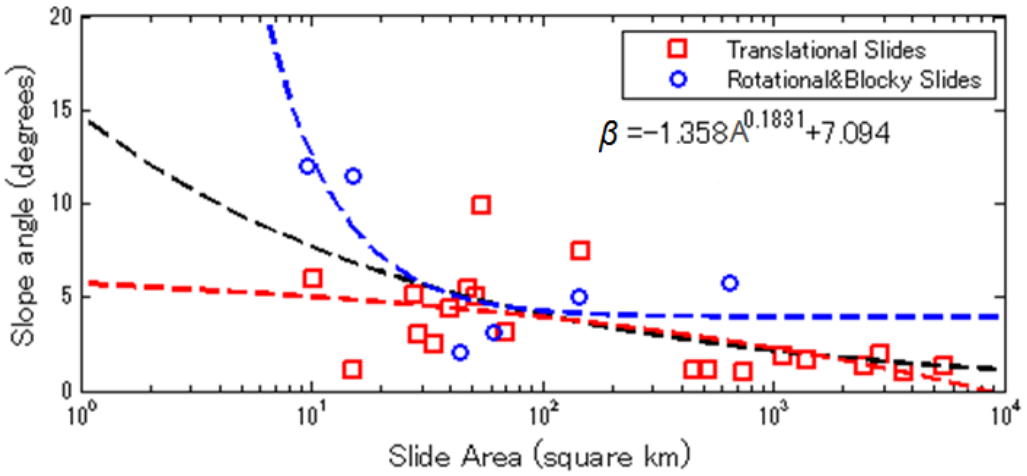

Figure 2.17: Empirical relationship between slope angle and slide area obtained from observed data. Fitting line for translation landslides (dashed-red), rotational and blocky landslides (dashed-blue), combined translation and rotational or blocky landslides (dashed-black).

Hence, it is assumed, that for any value of angle that is less than 5.024° the area is 10 km^2.

2.8 Width of the Submarine Landslide

The width of the submarine landslides along the transects cannot be determined from the MCS as it varies depending on the distribution of sediments and will be

distinct for each site. Hence, it is also empirically determined using the observed data ten Brink (2009), McAdoo (2000). When the area of the landslide is obtained as mentioned in the previous section, the width of the landslide is also determined empirically obtained by fitting the observed values of area and width of the existing landslides as shown in Figure 2.18. For any value of area from $1 - 10000$ km^2 the width of the landslide is given by the equation,

$$W = 2.32\ (\log A)^{1.85} \tag{2.10}$$

where W is the width of the landslide in km and A is the area of the landslide in km^2 determined empirically from equation of area calculated earlier.

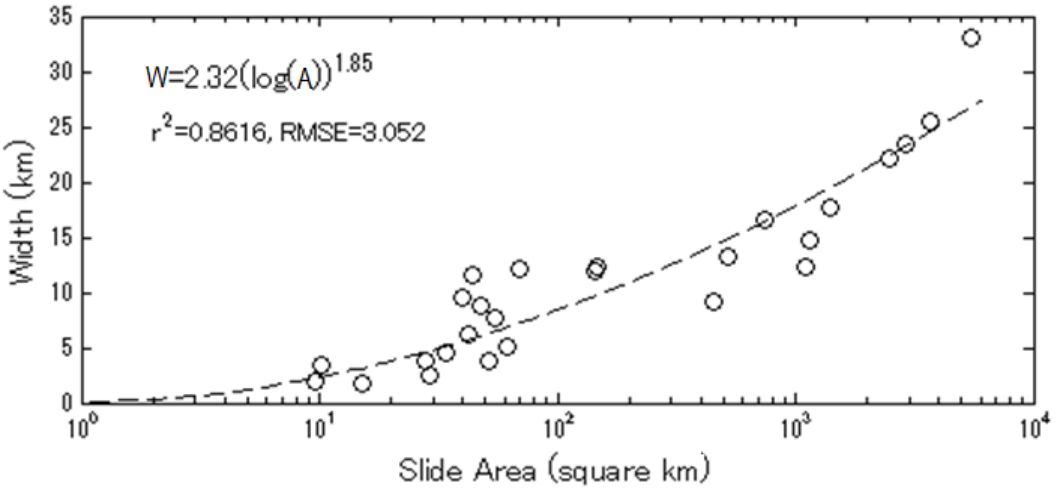

Figure 2.18: Graph showing the empirical relation between slide area and width of the landslide

2.9 Landslide Initial Tsunami

For every submarine landslide that occurs, a wave amplitude is generated. The initial amplitude of the wave generated is one of the most important characteristics for defining a tsunami wave. The determination of landslide initial tsunami wave for the GOM is based on the research result of landslide tsunami production in a 3-D Numerical Wave Tank by solving fully Non-linear potential flow equations for submarine landslides, Grilli et al., (2002). The equation of initial tsunami amplitude caused by translational landslide is determined at the center of the landslide and is given by the given the semi-empirical relation

$$\eta_o = S_o(0.0574 - 0.0431\sin\beta)(\frac{T}{l})(\frac{lsin\beta}{d})^{1.25}(1 - e^{-2.2(s-1)})(\frac{w}{w+\lambda_o}) \tag{2.11}$$

where, η_o is the initial amplitude depression of the wave generated due to submarine landslides, d is the water depth at the center of the landslide, w is the width of landslide, l is the length of landslide, t is the thickness of landslide, β is the slope of landslide, S_o is the characteristic distance of motion λ_o is the wavelength of tsunami wave.

The characteristic distance of motion and wavelength of the tsunami wave is given as follows:

$$S_o = \frac{\pi}{2}l(s+1) \tag{2.12}$$

$$\lambda_o = \sqrt{\frac{\pi ld(s+1)^2}{2sin\beta(s-1)}}. \tag{2.13}$$

All the η_o generated will not be responsible for causing a tsunami, hence the landslides that give rise to very small η_o should be eliminated. Therfore, a threshold value for the amplitude parameter is defined such that, all the values of η_o below the

threshold will be eliminated and the remaining values η_o thus obtained should follow a lognormal distribution.

2.10 Estimation of Return Period

The return period of the tsunami-genic submarine landslide is obtained as follows by the equation given, after removing all results where the initial wave amplitude is lesser than the threshold value,

$$P_F = \frac{n}{N} \tag{2.14}$$

$$P_{SL} = P_{PHA} P_F, \tag{2.15}$$

where P_F is the ratio of the number of tsunami-genic slope failures 'n' to the total number of trials across the transects N, P_{SL} is the joint probability of exceedance of the tsunami-genic submarine landslide as a result of seismic activity, P_{PHA} is the reciprocal of the PHA return period at which the tsunami-genic failure occurs, . The reciprocal of P_{SL} will give the return period of the tsunami-genic submarine landslide. The P_{SL} result will define the characteristic of the landslide related to the probability of exceedance to identify the large events for tsunami-genic landslides.

3. METHODOLOGY

The methodology used here is partly conceived based on the MCS model developed by Grilli et al., (2002), for the Upper East Coast of the United States. A flowchart of the probabilistic model used in this study is as shown in Figure 3.1.

The most important input required for the probabilistic model is the statistical distribution of the observed submarine landslides, the soil data along transect, and the PHA for the seismic activity taking place in the GOM. The first step in the generation of the probabilistic model is the selection of transects A, B, C and D located strategically at the continental shelf in the GOM. The slopes at these transects are obtained as mentioned in section 2.2 and the parameters depth(d), length (l) and thickness (T) for each the transects are determined individually by randomly generating them based on the distribution of the observed parameters as explained in section 2.3. When the random variable are generated they are checked to see if they fall within the limits of the existing landslides so that the output parameters are constrained within the limits of the observed data. When the length, depth and thickness of the landslide are obtained, the slope of the landslide is calculated using the Equation 2.8 and the area of the landslide is determined based on the Equation 2.9. The width of the landslide is found from the fitting Equation 2.10 which gives the relation of area and width. The thickness to the length ratio (T/l) is determined to see if they comply with the limits of the observed values (0.0003 - 0.07). In the process of generating any of the parameters (T, l, d and T/l) are not satisfied, the process is repeated.

The next step in the model is the determination of the stability of the slope using the Equation 2.7. The bulk density and shear strength data are obtained from the

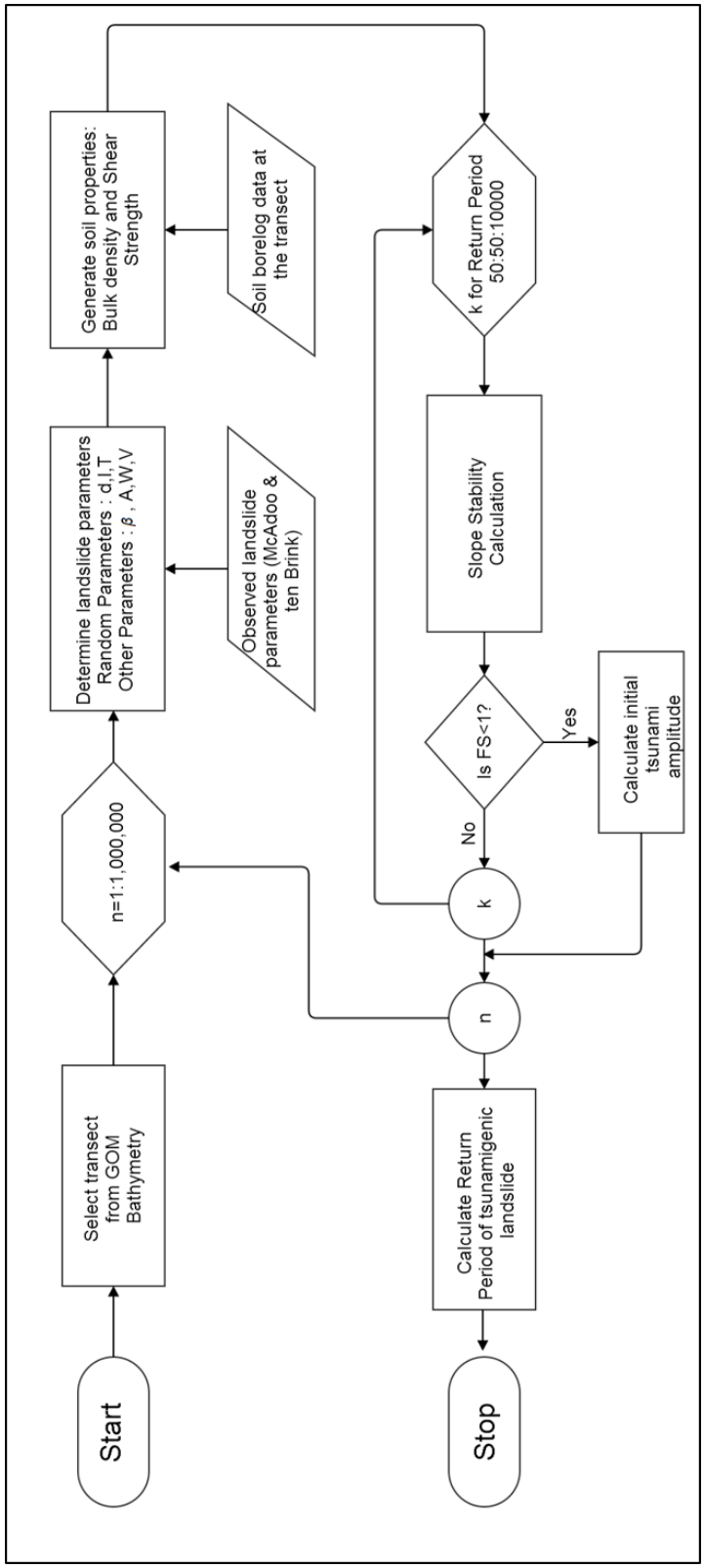

Figure 3.1: Flowchart showing the steps involved in the probabilistic model.

curve fitting equations determined from Appendix B depending upon the thickness of the landslide as shown in Figure 3.2 for the transect being analyzed. The slope stability analysis is carried out and if the factor of safety is less than one a landslide will occur. The slope stability analysis is carried out by determining the factor of safety (Equation 2.7). If the factor of safety is less than unity the landslide occurs, the initial tsunami amplitude is calculated. These steps are repeated 1000,000 times for each transect as explained in section 2.3 by Equation 2.3 to assure convergence.

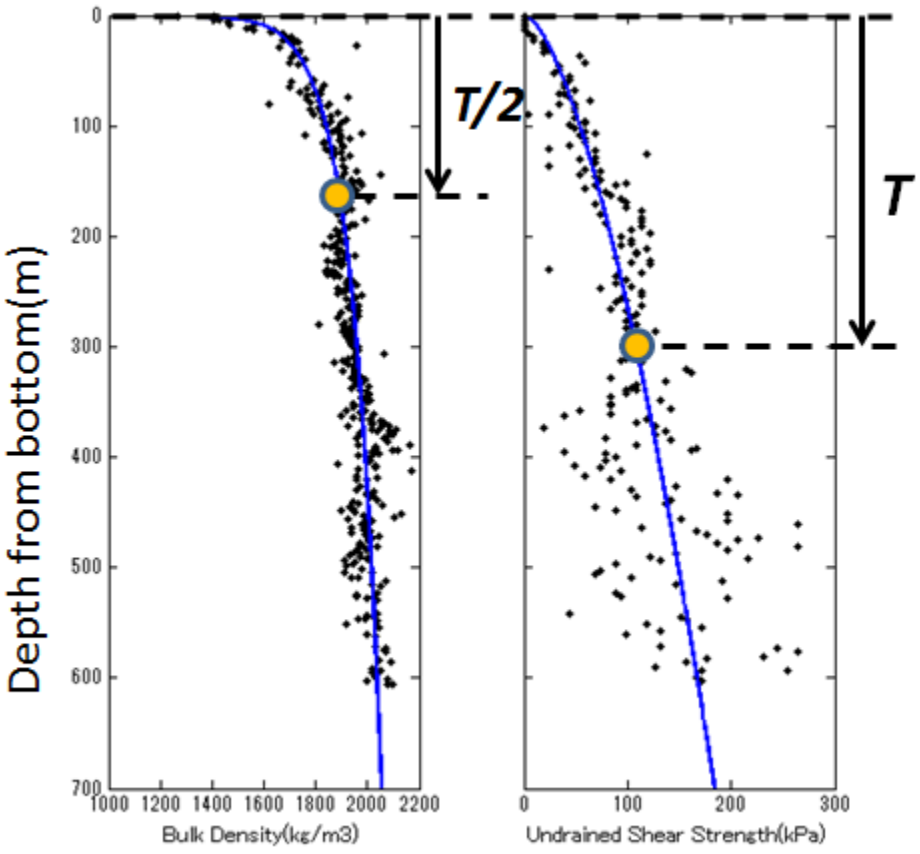

Figure 3.2: Locations at which bulk density and undrained shear strength are determined.

A threshold is imposed to limit the initial tsunami amplitude by using the best fit curve for the lognormal distribution. The threshold initial tsunami amplitude was obtained by comparing the cumulative distributive function with different threshold amplitude and verifying by trial and error the best fit with the lognormal distribution. The best fit correspond to the threshold of 0.02m as shown in Figure 3.3 which surprisingly is consistent with the results obtained from Grilli (2009). Figure 3.3 is an example of the cumulative frequency distribution of the initial tsunami amplitude for different threshold amplitude at transect C. The return period of the tsunami-genic landslide is obtained by determining the joint probability by using the Equation 2.15. All the results having a return period of more than 10,000 years are removed because according to the Equation 2.3 the probabilistic model is designed for a return period of 10,000 years for a maximum coefficient of variation 10%.

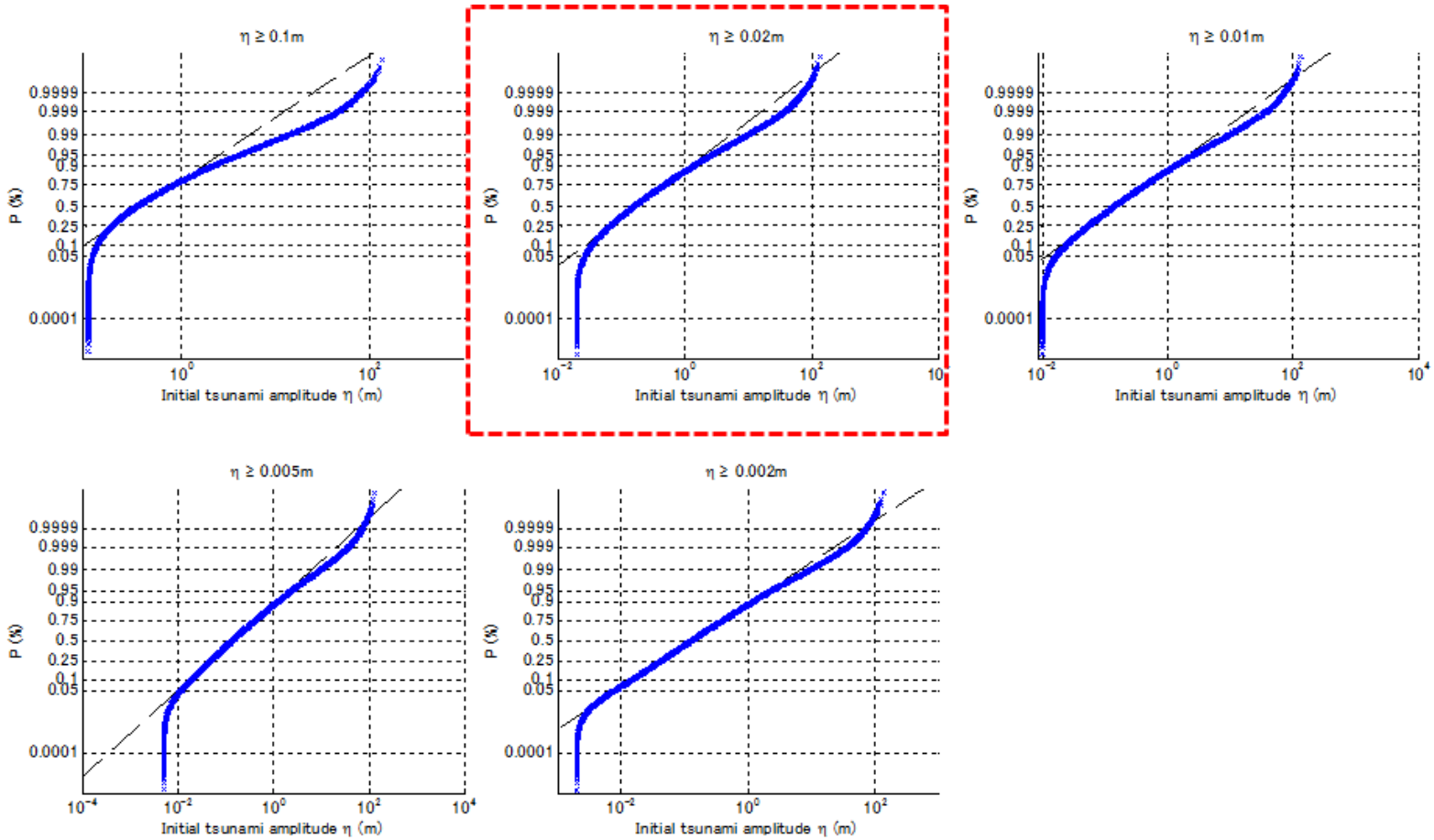

Figure 3.3: Finding the threshold amplitude by using the best fit curve for the lognormal distribution of the initial amplitude.

4. RESULTS

From the probabilistic model, the landslides that occur on each transect is determined along with their location, geometric parameters (l,d and T), slope, area, volume, initial amplitude of the wave generated by them and the return period at which they take place.

The most important result of the probabilistic model is the relationship between the return period of the tsunami-genic submarine landslide and the initial amplitude of the wave generated as a result of the submarine landslide. The results obtained are from 1000 to 1,000,000 years of period of recurrence. However, in our study we limited our results only up to 10,000 years of period of recurrence because the probability of occurrence of a tsunami-genic landslide beyond 10,000 years is very less. Figure 4.1 and 4.2 shows the relationship between the initial tsunami amplitude and the return period. The red dots in the Figure 4.1 represent the wave amplitude corresponding to maximum driving force for each return period on transect C and in the Figure 4.2 represent the wave amplitude corresponding to maximum amplitude for each return period. The result also emphasizes the fact that the maximum wave amplitude at each return period does not necessarily correspond to the maximum driving force which is a function of the mass. The relation of the inverse of depth that corresponds to the various return periods in Figure 4.2 clearly indicates that landslide in shallow water are more efficient in generating tsunamis.

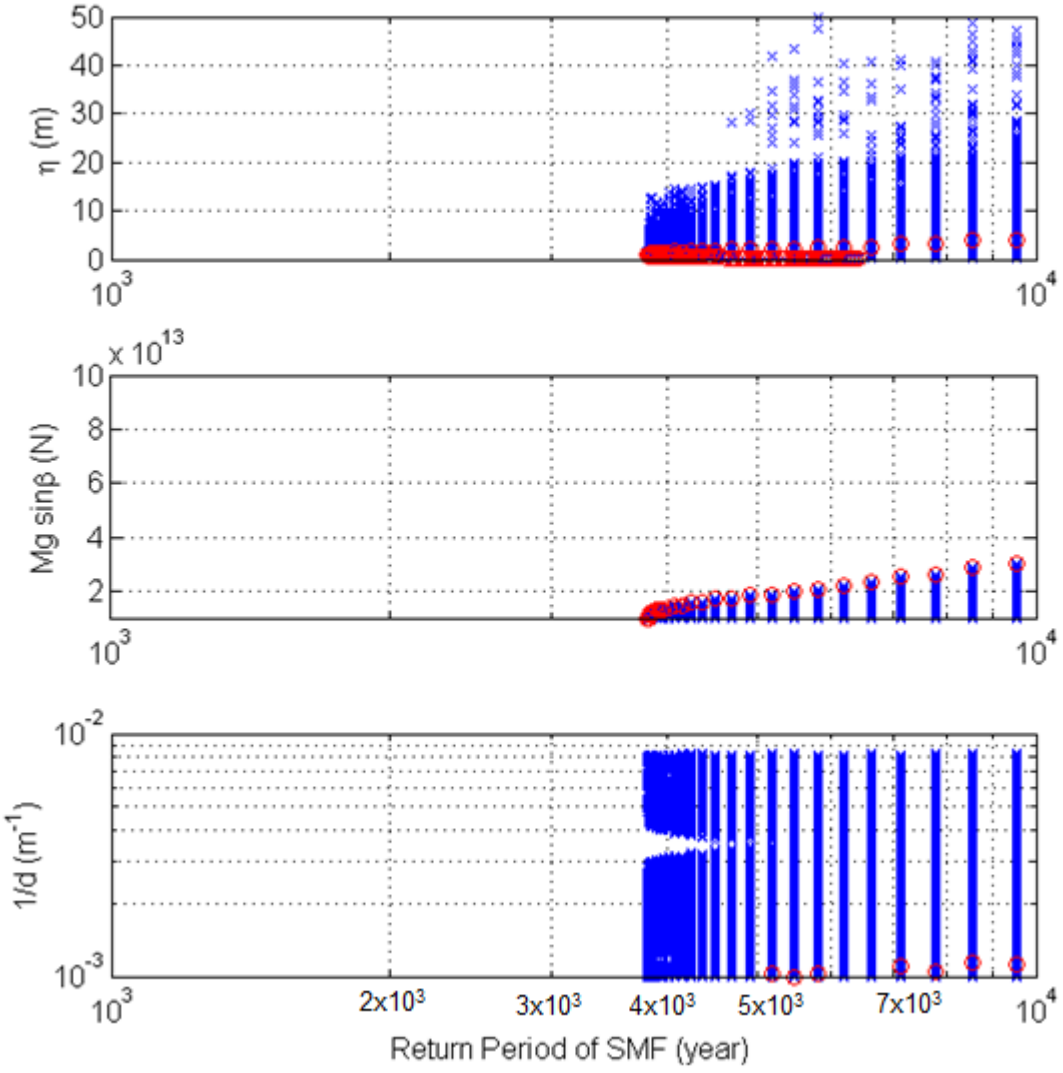

Figure 4.1: Initial wave amplitude generated by submarine landslide for different return period. Red dots represent wave amplitude corresponding to the maximum driving force.

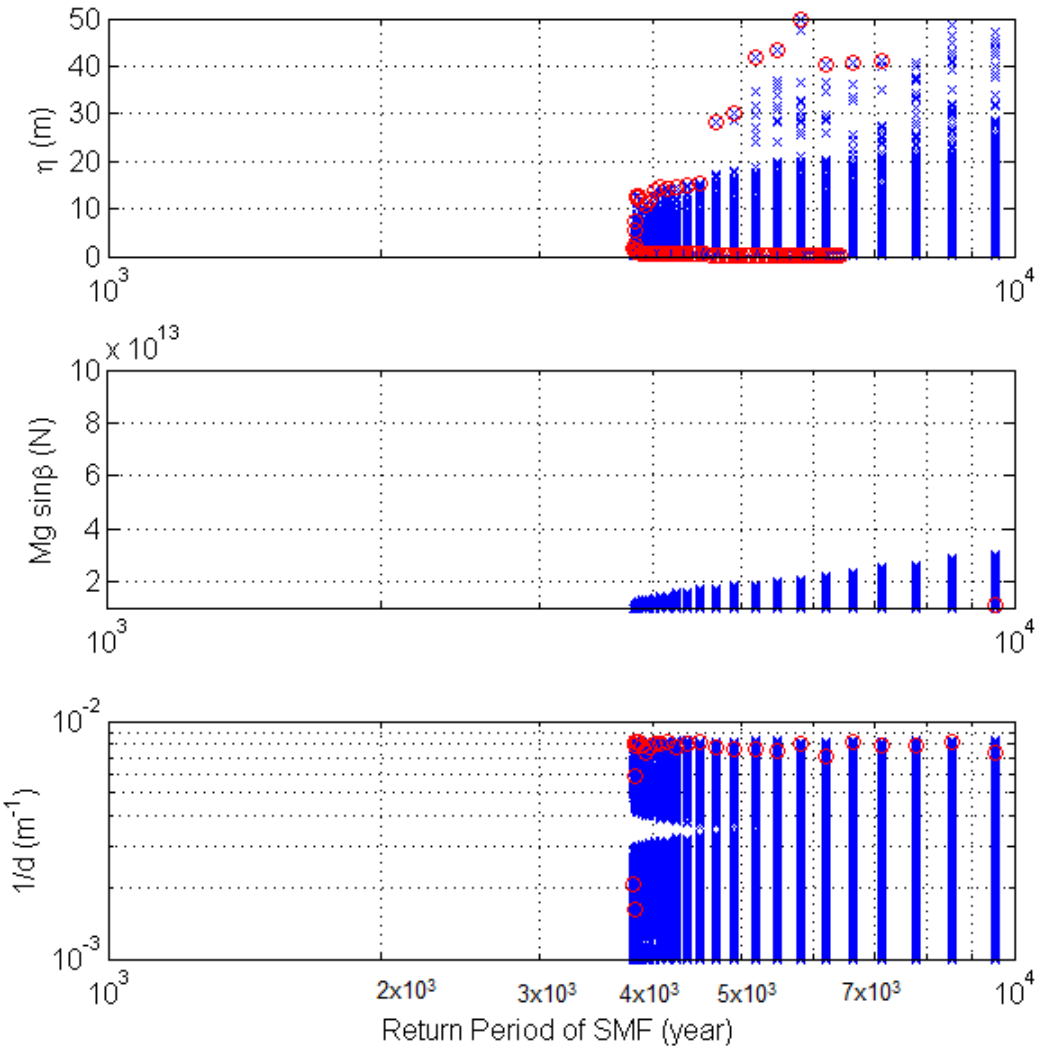

Figure 4.2: Initial wave amplitude generated by submarine landslide for different return period. Red dots represent wave amplitude corresponding to the maximum amplitude

5. VALIDATION

The validation of the probabilistic model depends upon the distribution of the parameters. Any error in the distribution will give unrealistic results. Hence, in this section a number of comparative studies between the observed data and the simulated values of the probabilistic method are performed to validate the model.

5.1 Comparison of the distribution of input and output parameters

The Monte Carlo Simulation Model generates a large number of submarine landslides with randomized parameters (like depth, location, runout length, headscarp height, width, slope, etc.) capable of producing tsunamis. Parameter values are validated to verify if their distribution follow the same distribution from observed landslide parameters. Figures 5.1, 5.2 and 5.3 show the distribution of the runout length (l), depth (d) and thickness (T) of the submarine landslides generated by the probabilistic model. The Chi-square test for the goodness-of-fit for these parameters showed a 95% confidence on their respective distribution.

5.2 Relation between landslide Volume and Area

Power law relationship between the landslide area and volume of observed and simulated parameters show consistent result as shown in Figure 5.4

5.3 Relation between landslide Volume and cumulative number of landslide failures

Comparing the slope for the relationship between landslide volume and cumulative number of landslide failures for both the observed and the generated data as shown in Figure 5.5, it is found that the slope is consistent with result obtained by ten Brink (2006) of 0.64.

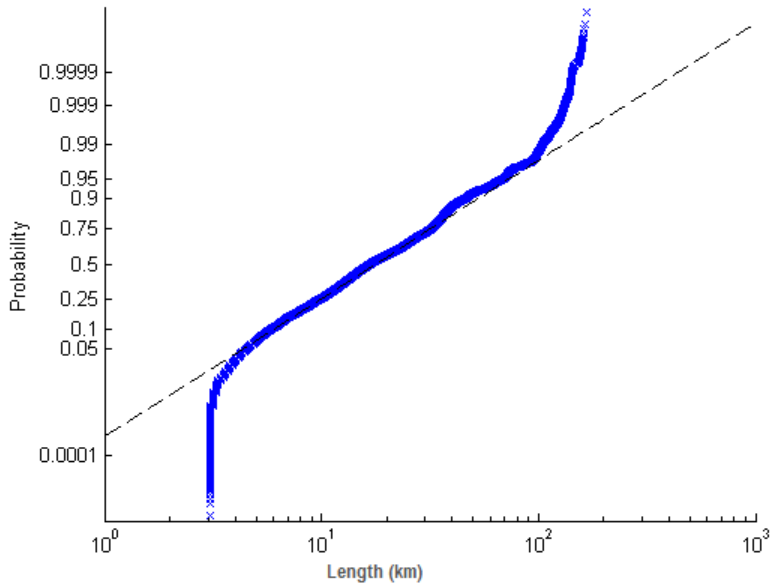

Figure 5.1: Probability plot of lognormal distribution of the landslide length generated by the model

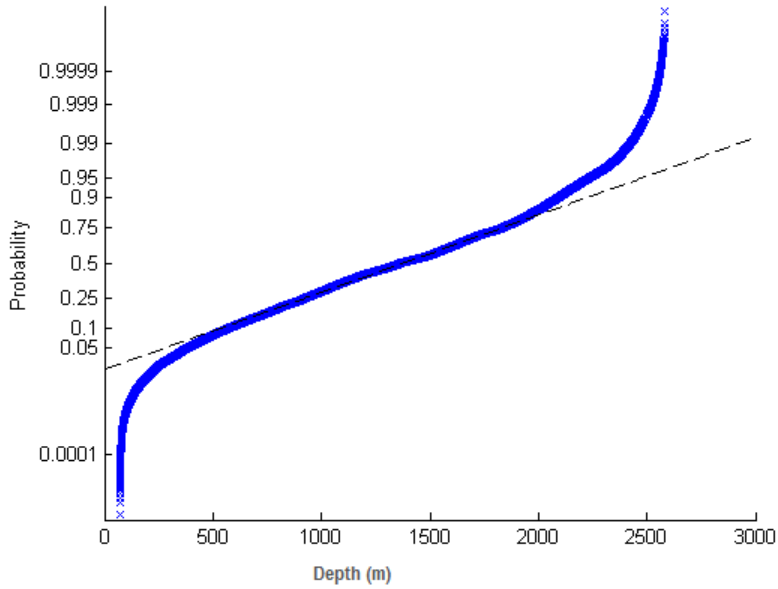

Figure 5.2: Probability plot of normal distribution of the water depth at which the landslide occurs generated by the model

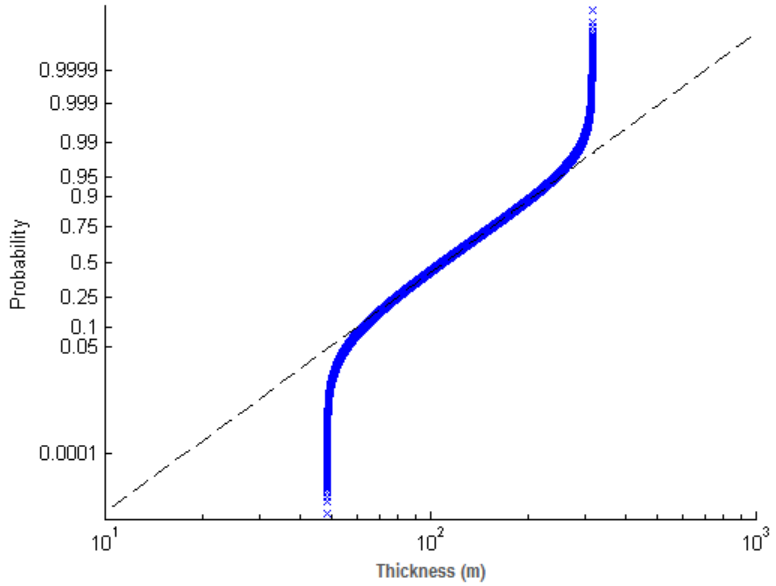

Figure 5.3: Probability plot of lognormal distribution of the landslide scarp height generated by the model

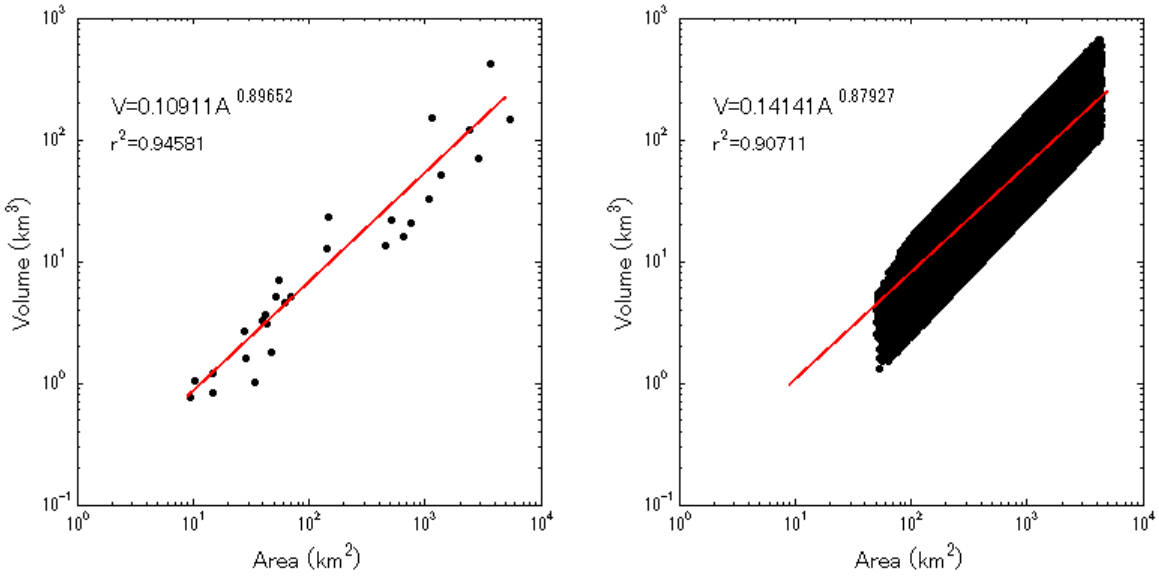

Figure 5.4: Relationship between the landslide area and volume of the observed data (left panel) and generated data by the probabilistic model (right panel)

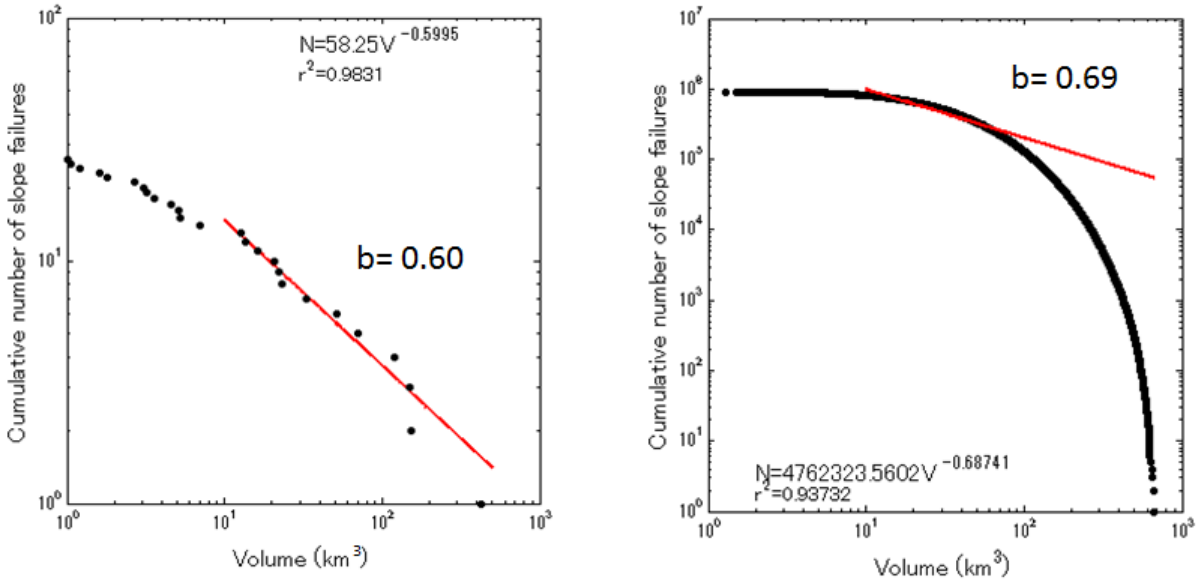

Figure 5.5: Comparison of slopes for the relationship between landslide volume and cumulative number of landslide failures of both, observed (left panel) and generated data (right panel)

6. CONCLUSION

A probabilistic model using MCS methodology has been developed to identify the submarine landslide sources and its parameters like location, depth of occurence, thickness, slope, width, area, volume, amplitude of the initial wave generated and the probability of exceedence of each landslide that may occur in the GOM along the specified transects. The results obtained from the probabilistic model have been verified and the parameters generated follow the same distribution as the observed parameters of landslide. Looking at the results of the initial amplitude of the wave generated, it is seen that they increase with the increase in return period of the tsunamigenic wave. Large scale tsunami waves occurs at shallower depth. Large values of driving force of the landslide (proportional to the mass of the landslide) do not always give large tsunami amplitude.

7. FUTURE WORK

The study can be further improved by increasing the number of transects work is so that there is a better coverage of the GOM and thus a better picture of the tsunami inundation caused in the GOM can be studied. More precise values of the soil characteristics like angle of internal friction (ϕ) and coefficient of cohesion (c) will help in solving the slope stability analysis, at the transects with more accuracy. The model can be improved to study about the submarine landslides and their corresponding waves that are generated due to rotational slope failures, that account for 21% of the landslides that occurred in the GOM.

BIBLIOGRAPHY

Amante, C., & Eakins, B.W. (2009). *ETOPO1 1 arc-minute global relief model: procedures, data sources and analysis.* US Department of Commerce, National Oceanic and Atmospheric Administration, National Environmental Satellite, Data, and Information Service, National Geophysical Data Center, Marine Geology and Geophysics Division.

Ang, A. H., & Tang, W. H. (2007). *Probability Concepts in Engineering: Emphasis on Applications in Civil & Environmental Engineering.* John Wiley & Sons, Inc.

González, F. I., Geist, E. L., Jaffe, B., Knolu, U., Mofjeld, H., Synolakis, C. E., & others (2009). Probabilistic tsunami hazard assessment at seaside, Oregon, for near and far field seismic sources. *Journal of Geophysical Research: Oceans (1978–2012)*, 114(C11).

Grilli, S. T., Taylor, O. D. S., Baxter, C. D., & Maretzki, S. (2009). A probabilistic approach for determining submarine landslide tsunami hazard along the upper east coast of the United States. *Marine Geology*, 264(1):74-97.

Grilli, S. T., Vogelmann, S., & Watts, P.(2002). Landslide Tsunami Amplitude Prediction in a Numerical Wave Tank. *Ocean Wave Measurement and Analysis (2001)*, 1495-1504.

Hammack, J. (1972). *Tsunamis: a model of their generation and propagation.* WM Keck Laboratory of Hydraulics and Water Resources, California Institute of Technology.

Horrillo, J.J., Wood, A., Williams C., Parambath A., & Gyeong-Bo, K. (2010),. Construction of tsunami inundation maps in the Gulf of Mexico. *Technical report, National Tsunami Hazard Mitigation Plan*,1-90.

IODP Management International, Inc., for the Integrated Ocean Drilling Program. (2008-09). Proceedings of the Integrated Ocean Drilling Program , Volume 308 expedition reports Gulf of Mexico Hydrogeology. *http://publications.iodp.org/proceedings/308/308toc.htm*

Knight, B. (2006). Model predictions of Gulf and southern Atlantic Coast tsunami impacts from a distribution of sources. *Science of Tsunami Hazards*, 24(5):304-312.

Locat, J., & Lee, H. J.(2002). Submarine landslides: Advances and challenges. *Canadian Geotechnical Journal*, 39(1):193-212.

Lynett, P. J., & Martinez, A. J. (2012). A probablistic approach for the waves generated by submarine landslide. *Coastal Engineering Proceedings*, 1(33):1-15.

McAdoo, B. G., Pratson, L. F., & Orange, D. L. (2000). Submarine landslide geomorphology, US continental slope. *Marine Geology*, 169(1):103–136.

Milne, J. (1886). Earthquakes and other earth movements. *Kegan Paul, Trench and Company*.

NOAA National Geophysical Data Center. (2008). NOAA/WDS Global Historical Tsunami Database. *http://www.ngdc.noaa.gov/hazard/tsu_db.stml*

Priest, G. R., Goldfinger, C., Wang, K., Witter, R. C., Zhang, Y., & Baptista, A. (2009). Tsunami Hazard Assessment of the Northern Oregon Coast: A Multi-Deterministic Approach Tested at Cannon Beach, Oregon. *Oregon Department of Geology and Mineral Industries*.

Synolakis, C. E., Bardet, J. P., Borrero, J. C., Davies, H. L., Okal, E. A., Silver, E. A., Tappin, D. R. & others. (2002). The slump origin of the 1998 Papua New Guinea tsunami. *Proceedings of the Royal Society of London. Series A: Mathematical, Physical and Engineering Sciences*, 458(2020):763–789.

Tappin, D. R., Watts, P., & Grilli, S. T. (2008). The Papua New Guinea tsunami of 17 July 1998: Anatomy of a catastrophic event. *Natural Hazards & Earth Sciences*,

8(2).

ten Brink, U., Twichell, D., Lynett, P., Geist, E., Chaytor, J., Lee, H., Flores, C. & others. (2009). Regional assessment of tsunami potential in the Gulf of Mexico. *US Geological Survey Administrative report*.

ten Brink, U., Geist, E. L., & Andrews, B. D. (2006). Size distribution of submarine landslides and its implication to tsunami hazard in Puerto Rico. *Geophysical Research Letters*, 33(11).

APPENDIX A

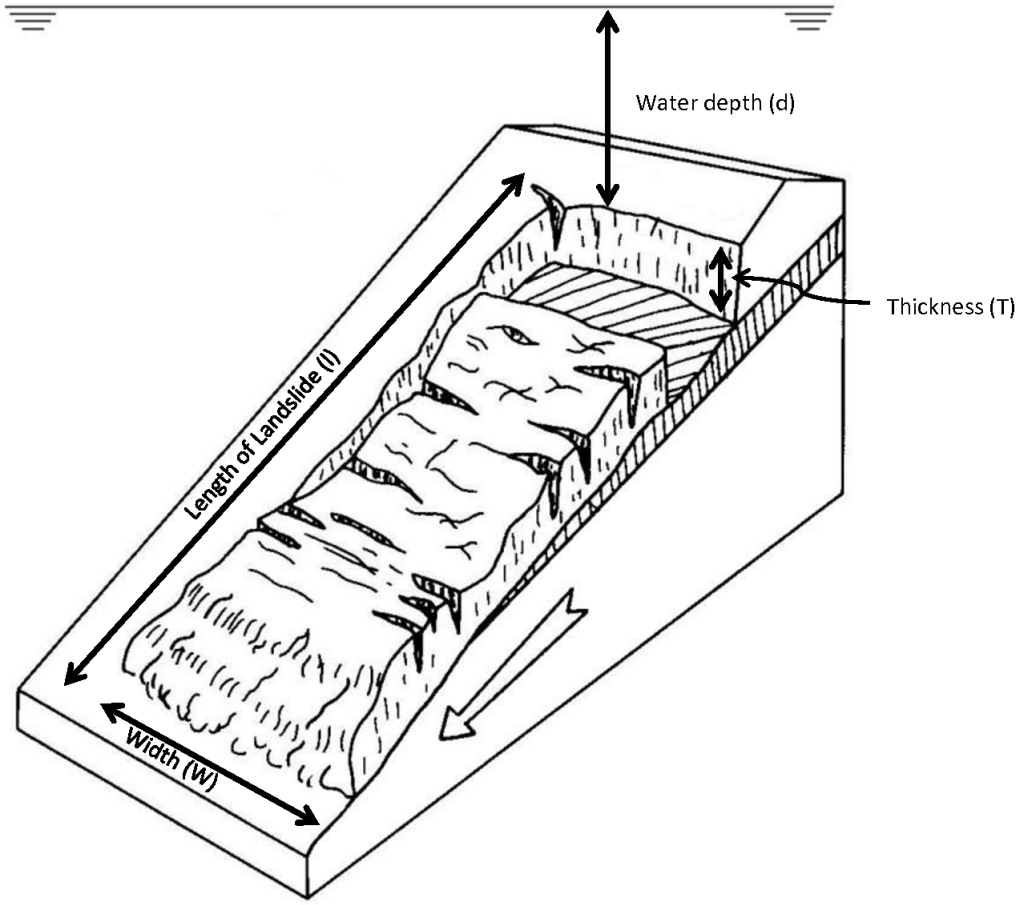

Figure A.1: Morphology of a Submarine Landslide

APPENDIX B

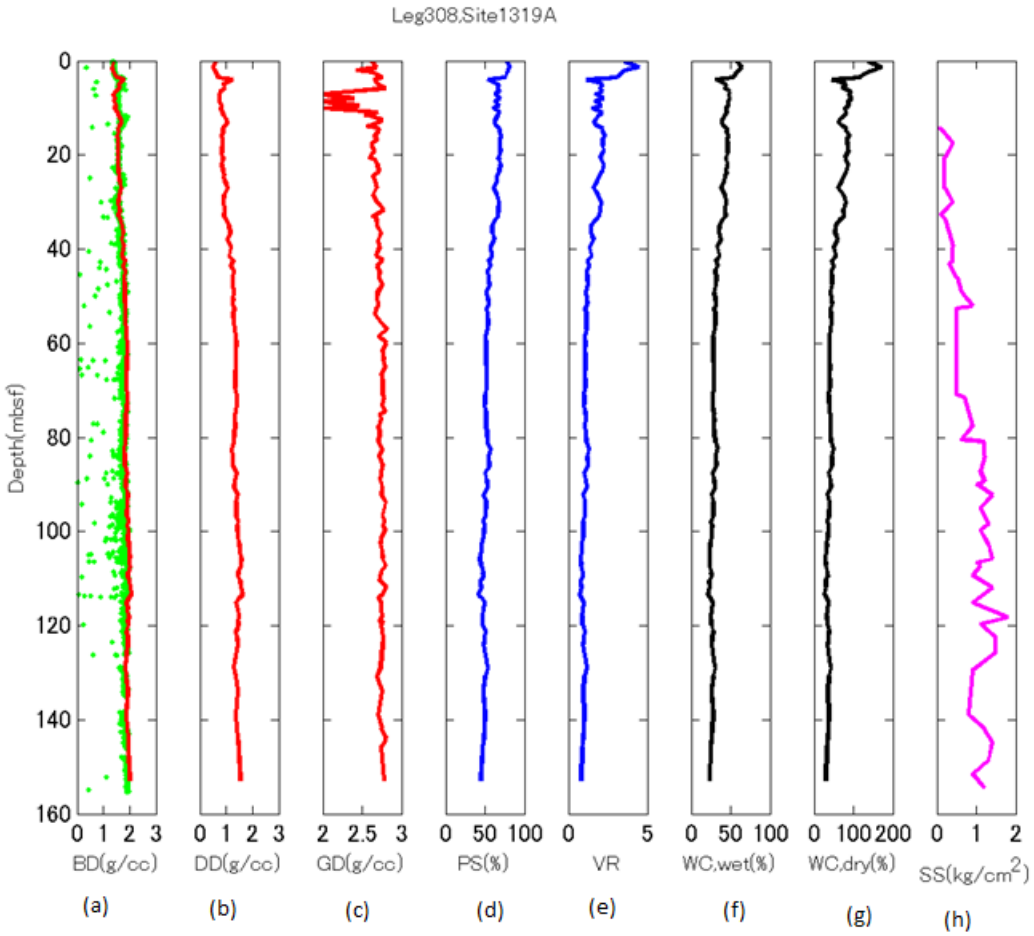

Figure B.1: Soil characteristics at Leg 308, Site 1319A

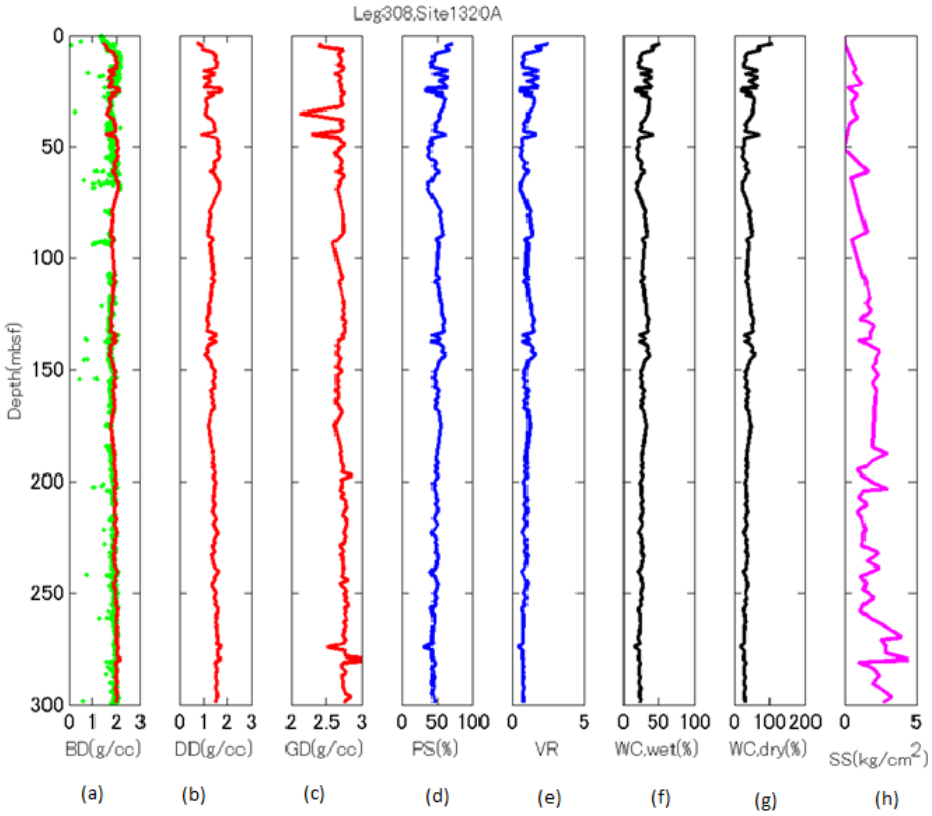

Figure B.2: Soil characteristics at Leg 308, Site 1320A

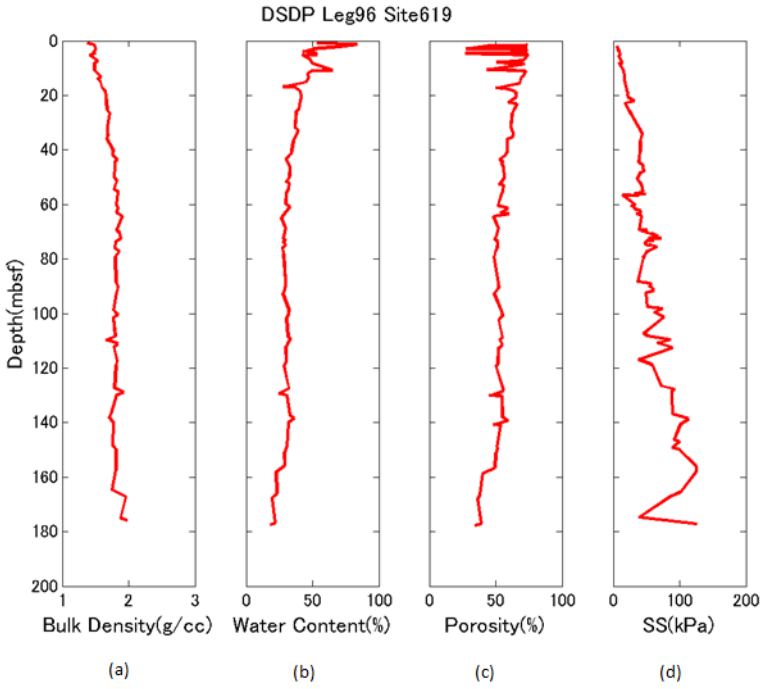

Figure B.3: Soil characteristics at Leg 96, Site 619

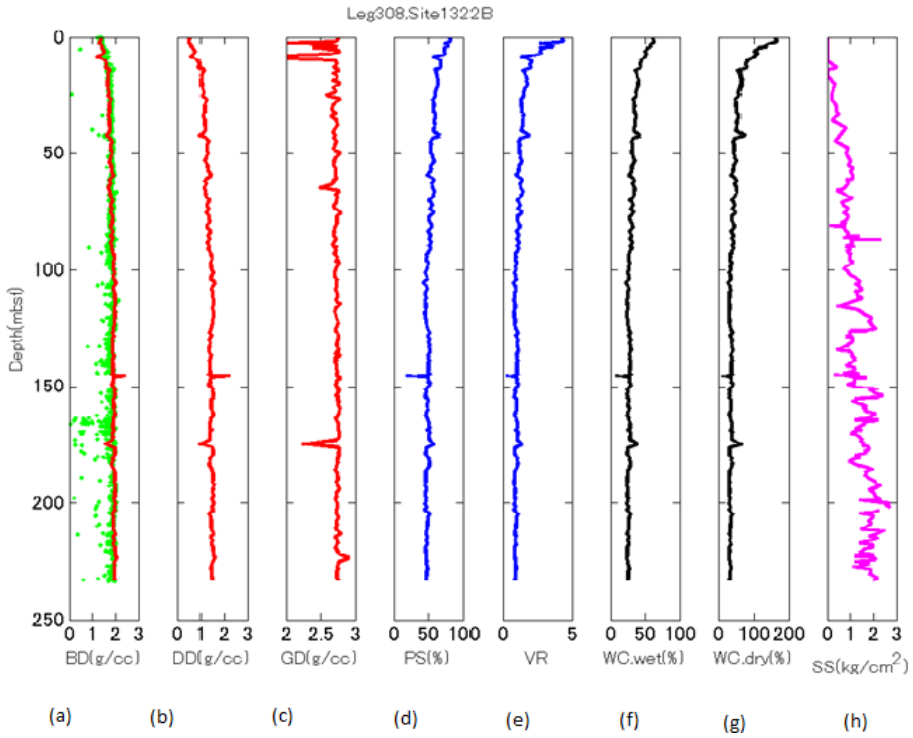

Figure B.4: Soil characteristics at Leg 308, Site 1322B

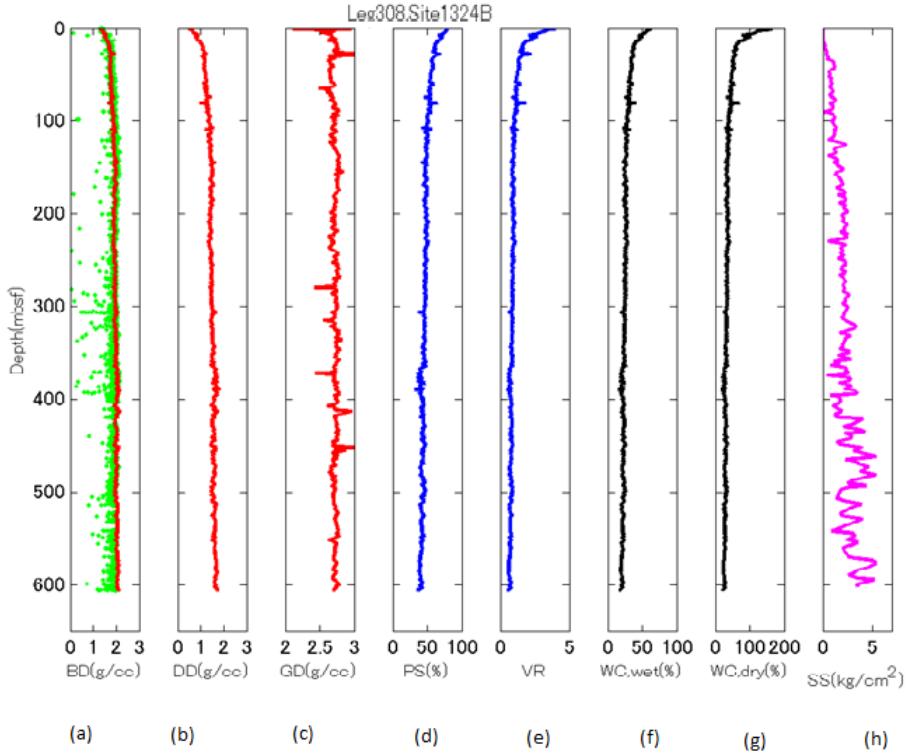

Figure B.5: Soil characteristics at Leg 308, Site 1324B

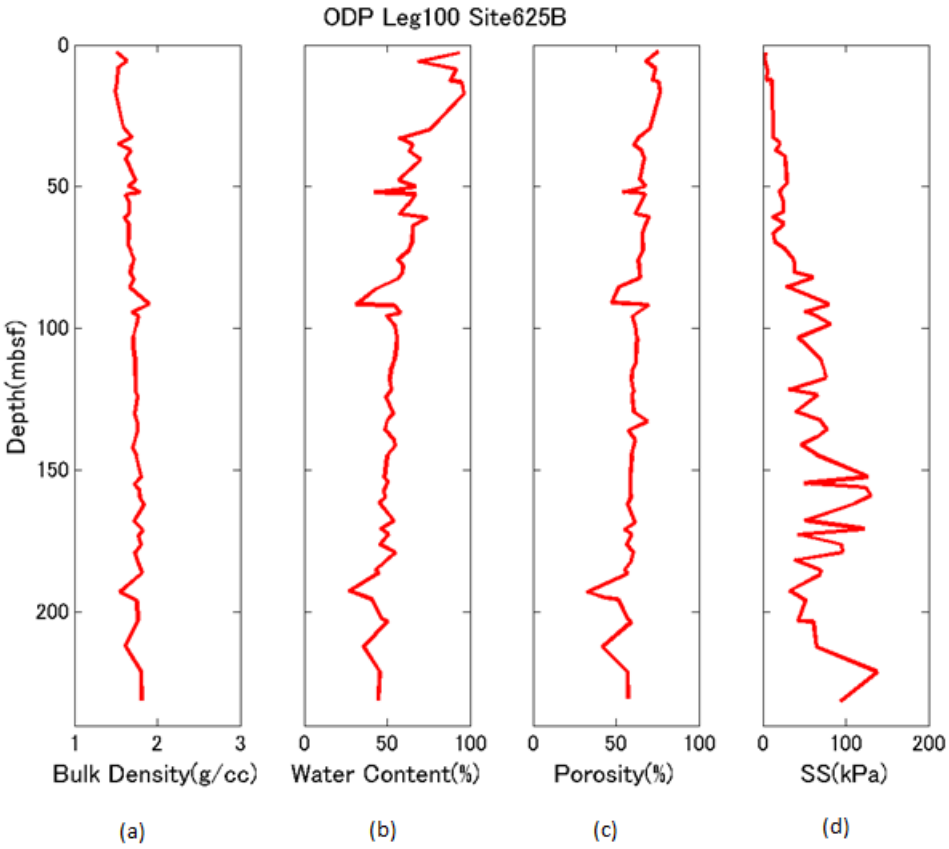

Figure B.6: Soil characteristics at Leg 100, Site 625B

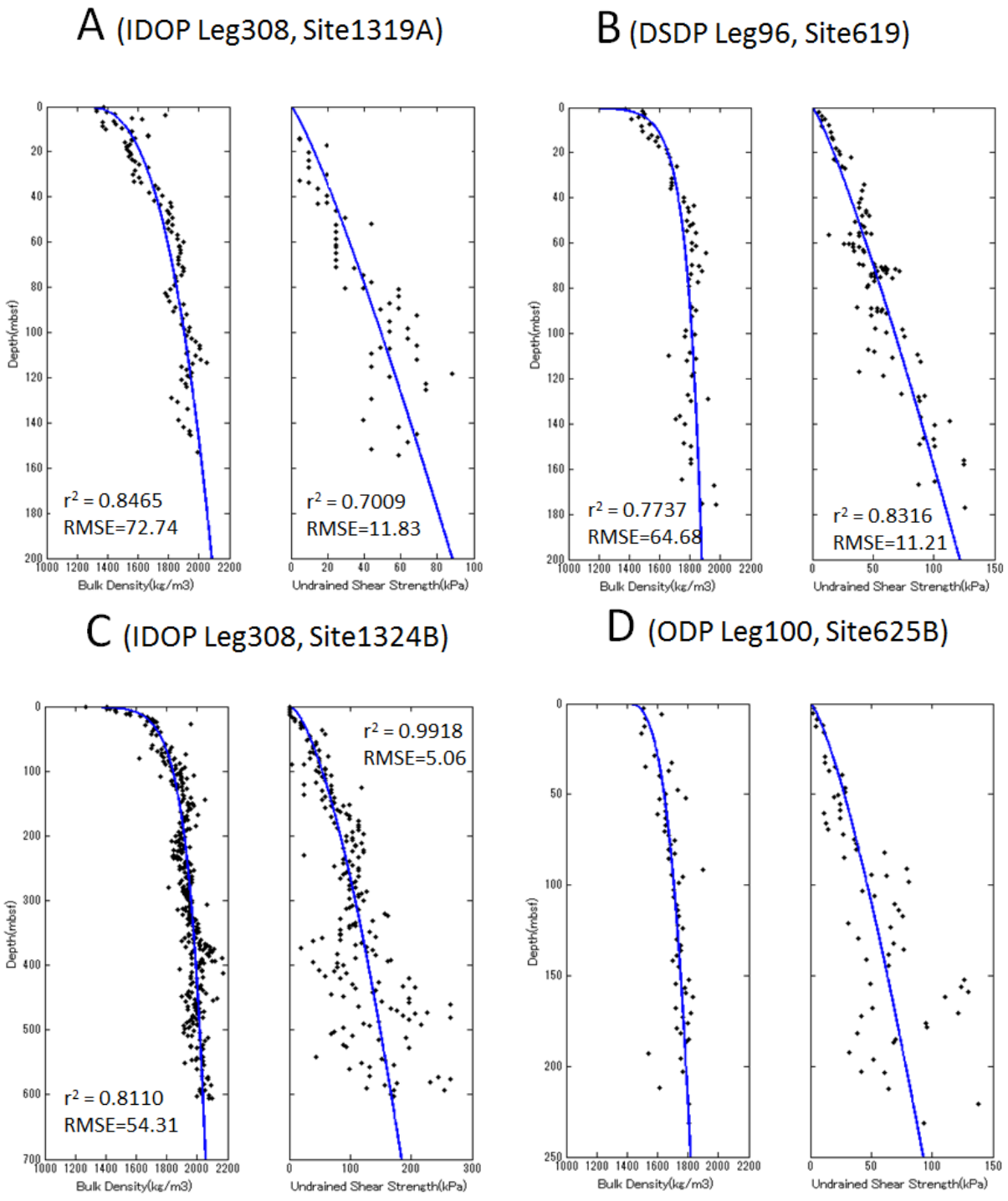

Figure B.7: Curve fit for Bulk Density and Undrained Shear Strength at Transect A, B, C and D